Forecasting Lives Lost to Climate Change – A Review

Authors and Affiliations

1. Mr Nigel Howard, Principal Clarity Environment, Beacon Hill, Sydney, Australia
2. Professor Peter Newman, John Curtin Distinguished Professor of Sustainability, Curtin University, Perth, Australia

Acknowledgements

The authors draw on and acknowledge the organisations and individuals that develop and make their data publicly available and quotes from publicly available papers as indicated and hyperlinked in the text. The authors wish to acknowledge the Centre for Research on the Epidemiology of Disasters, Institute of Health and Society, University of Louvain for their 50 years of compilation of the EMDAT disaster data that much of this study relies upon.

Authors' information

Nigel Howard FRSC is a chemist by training who has dedicated his career and now into retirement to using scientific methodology to promote change toward a climate safe future. He has worked in senior technical roles in government, NGO's and consultancy in the UK, US and now in Australia. He is a former Director of the Centre for Sustainable Construction (UK), a former Vice President of the US Green Building Council, former President of Australian Life Cycle Assessment Society and founded the Edge Environment Consultancy (AU)(Now Edge Impact International). He is an expert in Life Cycle Environmental Impact Assessment, energy and climate impacts from buildings, infrastructure and transport and has pioneered work in Buildings, Infrastructure, Materials and Product ecolabelling. He believes that scientific method can be applied to any field.

Peter Newman is the Professor of Sustainability at Curtin University and before that he was a Murdoch University foundation academic from 1974 until 2007 where he began in Environmental Science and finished as Director of the Institute for Sustainability and Technology Policy. In 2001-3 Peter has written 24 books and over 440 papers on sustainable cities and decarbonization policy. He created the term automobile dependence in the 1980's which is now standard terminology in urban planning and his book with Jeff Kenworthy has been called 'one of the most influential planning books of all time'. Peter has worked to deliver his ideas in all levels of government having been an elected councillor, seconded to advise three Premiers in Western Australia (1986, 1989, 2001-3) and on the Board of Infrastructure Australia 2008-14. He has been involved in IPCC for fifteen years as a Lead Author on Transport and on Cities. In 2014 he was awarded an Order of Australia for his contributions to urban design and sustainable transport. In 2018/19 he was the Western Australian Scientist of the Year. His latest national research project with Josh Byrne and CRC RACE is Net Zero Precincts which shows how cities can help create the new economy.

Forecasting Lives Lost to Climate Change – A Review

Abstract

This review synthesises empirical evidence linking global mean surface temperature to climate mortality through undernourishment, heat, extreme events, conflict, and disease, and introduces an exploratory precautionary metric: cumulative climate-related deaths per cumulative megatonne of greenhouse gas emissions (CO_2-e), intended to support policy evaluation under deep uncertainty. Using observed CO_2-driven warming relationships and globally available population vulnerability data, we estimate that continued business-as-usual emissions would impose very large, geographically concentrated mortality burdens this century, with risks escalating nonlinearly beyond 2 °C. While uncertainty remains substantial, especially for undernourishment and conflict pathways, the direction and scale of risk are robust, providing a broad exploratory framework for approximating climate-related mortality. Expressing mortality per Mt CO_2-e allows the metric to be applied across all greenhouse gases and policy contexts. The resulting estimates should be interpreted as scenario-based approximations contingent on the assumptions and historical relationships used in the model. The results imply that treating climate change primarily as an economic externality understates its consequences, and that precautionary policy assessment should explicitly account for human lives at risk or saved due to decarbonization. (Full derivation provided in Supplementary Information S3).

Keywords

climate mortality; food security; conflict reduction; disaster risk; emissions pathways; policy evaluation metric; net zero certification and assessment.

1. Introduction

Since 1990, the Intergovernmental Panel on Climate Change (IPCC) has assessed the science of climate change, adaptation, and mitigation, yet it has not provided systematic estimates of climate-related mortality (Shukla, Skea et al, 2022). This paper addresses that gap by reviewing prior approaches and proposing a simplified method to approximate global deaths attributable to climate change, past and future, based on atmospheric CO_2 concentrations and global mean surface temperature (GMST). Our aim is to highlight the human implications of climate change, beyond economic measures, and to introduce a metric of lives lost or saved that can be applied to policies, projects and investments.

Scientific concern over the climate emergency has grown steadily. In 2020, over 11,000 scientists from 153 countries issued a public declaration of emergency (Ripple, Wolf et al, 2020). Rising GMST, more frequent extreme weather events, and intensifying disasters have outpaced expectations (Chang, 2024).

Evidence consistently links atmospheric and oceanic warming with shifts in weather patterns and growing climate extremes (Ripple, Wolf, Gregg et al, 2023). Progress toward global emissions reduction has been slow (UNFCCC, 2022) with emissions continuing to grow at an average of 2.2%/yr between 2005 and 2015 (Le Quéré & Andrew, 2018), but after the Paris Agreement in 2016 emissions growth has begun to slow (Friedlingstein & O'Sullivan, 2023) as exponential increase in adoption of renewables has begun (Newman, 2025). Over 1,500 climate laws and policies exist worldwide (Nachmany & Setzer, 2018). The EU has legislated climate neutrality by 2050 (Erbach, 2021) In its 23 July 2025 Advisory Opinion on the Obligations of States in Respect of Climate Change, the ICJ unanimously affirmed that states have significant obligations under international law relating to climate mitigation and prevention of serious environmental harm. None of this has been enabled by a metric that can account for climate-related mortality.

Public recognition of climate risk is increasingly using language that considers climate change an emergency (Fisher & Snow, 2021), and by 2024 at least 23 national governments plus the EU had issued emergency declarations (Climate Emergency Declaration, 2024). Human rights organisations have framed anthropogenic global warming (AGW) as a violation of fundamental rights (Caney, 2017), while health scholars warn of dire implications for food security, disease, and safe air and water (Watts, Amann et al, 2018). The right to a healthy environment is now constitutionally recognised in 118 countries (Kravchenko, 2007), and the UN Convention on the Rights of the Child obliges states to safeguard children's survival and development (United Nations General Assembly, 1989). Climate-related mortality is therefore becoming a necessary part of climate policy.

Climate litigation has emerged as one mechanism of climate accountability. By 2020, at least 1,550 climate-related court cases had been filed in 38 countries and EU courts, nearly doubling since 2017 (Burger & Tigre, 2023) though no certification process has yet suggested climate-related human mortality assessments be included.

Despite widespread recognition of climate risks, relatively little work has quantified the number of lives already lost, or likely to be lost, due to climate change. Previous analyses have focused primarily on economic damages, with human mortality largely overlooked. Nolt has argued that the mortality costs of climate change far exceed economic losses (Nolt, 2011), yet this perspective has not been integrated into mainstream assessments, perhaps due to the lack of statistical veracity. Developing mortality metrics is therefore necessary to help clarify the consequences of actions and policies, enabling accountability for deaths associated with continued emissions and for recognition of lives saved by mitigation.

This paper proposes one such metric, estimating global deaths attributable to climate change across multiple impact categories and relating them to cumulative CO_2 emissions. While correlations cannot alone establish causation, CO_2 concentration is the internationally accepted indicator of anthropogenic climate forcing and provides a reasonable basis for high-level mortality estimation.

In taking this approach, we seek to open a neglected but vital conversation: quantifying mortality as a central measure of climate impact. Such estimates, even with significant

uncertainties, can support precautionary action, inform policy design, and strengthen accountability mechanisms.

This paper is intended as an exploratory and precautionary systems-level synthesis rather than a definitive causal attribution model. The objective is not to predict exact future mortality outcomes, but to investigate whether large-scale empirical relationships, interpreted alongside established physical climate mechanisms and vulnerability pathways, can provide useful approximations of the potential human consequences of alternative emissions trajectories. Given the potentially existential scale of climate risks, the authors argue that approximate mortality estimation under uncertainty may still provide policy-relevant insight where no integrated framework currently exists.

2. Methodology

Detailed methodological descriptions, regression specifications, scenario assumptions, and extended data tables are provided in the Supplementary Information (SI).

In order to approximate global mortality attributable to climate change and to estimate lives lost per megatonne of CO_2-equivalent emissions, the mortality categories assessed include starvation, conflict, storms, floods, landslides, droughts, wildfires, epidemics, extreme temperatures, malaria, and diarrhoeal disease.

Earthquakes and volcanic activity were considered but excluded since the apparent trend with atmospheric CO_2 concentration was no longer evident when incidents were expressed per-capita of human population The apparent trend is more likely due to increasing population exposed coincidental to increasing CO_2 concentration rather than due to changes in climate. This is supported by the Centre for Research on the Epidemiology of Disasters (UNDRR & CRED, 2020) & and by IPCC (IPCC, 2021).

Future projections are developed under four emissions pathways: net zero by 2050 (Paris Agreement target), and two ‘postponed pathways’ net zero by 2060 and net zero by 2070, as well as a business-as-usual trajectory of continued emissions growth.

2.1 Literature and Data Review

A literature survey was conducted to identify the main mechanisms by which climate change contributes to human mortality, prior attempts to quantify deaths at the global scale, and areas of conflicting evidence (key findings in section 3.1). Publicly available historic datasets (1900–present) were compiled from international agencies including FAO (FAO, 2025), WHO (WHO, 2023), World Bank (World Bank, 2024), UN (United Nations, 2023), and EM-DAT, the international disaster database. (CRED, 2023). These datasets provided the empirical basis for correlating climate drivers—principally atmospheric CO_2 concentrations and global mean surface temperature (GMST)—with observed mortality outcomes.

2.2 Scenario Framework

Future deaths were modelled under the four emissions scenarios:

- Net zero by 2050 (Paris-aligned),
- Net zero by 2060,
- Net zero by 2070, and
- Business-as-usual (BAU), assuming continued emissions growth.

Population projections were based on the 2024 UN forecasts (United Nations, 2024), adjusted annually for climate-related mortality. In the BAU scenario, population decline from climate impacts becomes the main mode for reducing emissions, whereas in the mitigation scenarios emissions are modelled with an S-curve emissions reduction trajectory to zero at the corresponding date. Atmospheric CO_2 concentrations were estimated year-on-year, accounting for natural carbon drawdown (through ocean dissolution, through photosynthesis and through mineralisation) with a composite half-life of ~72 years (Moore & Braswell, 1994).

2.3 Empirical Forecasting of Climate

Rather than relying on complex integrated assessment models, this study extrapolated empirical relationships from historical data. Linear regressions were developed linking:

- population (United Nations, 2024) to emissions (Ritchie, Rosado et al, 2023),
- cumulative CO_2 emissions (net of drawdown) to Atmospheric CO_2 Concentration (NASA, 2024) and
- Atmospheric CO_2 Concentration (NASA, 2024) to temperature anomaly and GMST (NASA, 2022).

These relationships provided the basis for forecasting mortality through to 2200.

2.4 Undernourishment and Conflict Deaths (see Supplementary Information S3, Eqs. S1–S13).

The World Food Programme (United Nations, 2021) estimated that in 2021, of the 740 million people suffering undernourishment, 9 million people (~1.2%), mostly children, died. This proportion was applied to the forecast undernourishment rates to estimate mortality. Undernourishment related deaths emerged as the dominant category of climate mortality, with conflict strongly intertwined. The effect of climate change on food production is well established (Hultgren et al., 2025), but wealthy nations and individuals can afford to buy food even when their nation's agriculture is compromised (see below and supplementary information S2.4).

Deaths from undernourishment and battle deaths were combined for this modelling. A dual-empirical curve model was therefore developed to iteratively best fit the combined available undernourishment and battle deaths (see Results 3.3):

- A declining trend in undernourishment with time (Uy (%)), reflecting global development (improved nutrition, reduced poverty)
- An increasing trend in undernourishment linked to rising CO_2, representing the climate-driven impacts that we are attempting to determine.

For the global data, these opposing curves intersect around 2017, where the inferred climate-related signal may begin to offset development gains.

Global aggregate relationships alone may overstate future undernourishment mortality in some regions because vulnerability differs substantially by latitude, economic capacity and food-import resilience. It will not automatically be the case that continuing climate change will affect all regions equally for both of these reasons. Accordingly, for this study, the same iterative dual-empirical methodology was applied to the available regional undernourishment (and conflict) mortality data from 2000-2023. This results in a set of regional factors (linearized S-curve gradient and intercept). These factors have then been linearly correlated with latitude (but with wide confidence limits), enabling an approximate model for the s-curve of potentially climate related undernourishment which was used for all regions where data is missing or where the region has been economically insulated from climate related undernourishment to-date. As climate change intensifies, this provides a tentative basis for exploring how additional regions may become progressively exposed to climate associated undernourishment.

In addition, global and regional data have been compiled for GDP/capita and the compound rate of growth (or decline) with time. Similar data have been compiled for the median and 10% poorest daily incomes (See Supplementary Information Figure S3). These data have been used to infer (assuming normally distributed) the standard deviation of incomes (See Supplementary Information Figure S4). Since we know the proportion of undernourished people by region, we can now estimate the income level that corresponds to the same proportion of the population being undernourished (See Supplementary Information Figure S5). This provides a threshold income above which citizens can afford imported food to mitigate any short-fall in regional food production, and beneath which citizens will be exposed to undernourishment (See Supplementary Information Figure S6). Using the regional compound rate of GDP growth compared to the global rate of GDP growth, we can infer how each region is becoming relatively more or less prosperous. This provides 4 regional conditions:

- Undernourished and getting relatively poorer – no chance of escaping (Regions in Africa and parts of Asia)
- Undernourished and getting relatively richer – undernourishment decreasing with increased prosperity (Regions in parts of Asia and Central America)
- Not undernourished yet but becoming relatively poorer – approaching the income threshold which cannot protect increasing proportions of the poorer citizens from undernourishment in climate vulnerable regions (Some European Regions and eventually North America)
- Not undernourished and becoming relatively wealthier – regions where the population is economically protected from food insecurity even when that region

starts to become climate vulnerable (Especially the emerging economies in parts of Asia)

We then related this to each region's income distribution to estimate the proportion of regional population that is economically exposed to undernourishment. The forecast proportion of undernourishment for each region is then taken as the minimum of the estimated exposure due to climate change or the estimated proportion of population vulnerable.

2.5 Disaster-Related Deaths

The EM-DAT database (CRED, 2023) was analysed to identify disaster classes significantly correlated with atmospheric CO_2. Storms, floods, landslides, and wildfires showed robust associations, while earthquakes, volcanic eruptions, and droughts (to avoid double-counting starvation) were excluded. Regression analysis estimated both disaster frequency and, where plausible, severity (deaths per disaster). Outliers were removed to test whether severity of impacts is increasing with climate change, not just frequency of disasters – severity appears not to be increasing. Population-normalised data helped distinguish climate drivers from population exposure effects.

2.6 Health Impacts

Climate-attributable deaths from heat and cold extremes, diarrhoea and malaria were reviewed but excluded due to insufficient or inconsistent correlation with CO_2 or GMST in the available data. The entire WHO database was downloaded, harmonised and recoded consistently for (750) medical conditions and reviewed for potential climate correlation.

2.7 Air Pollution

Air pollution deaths from fossil fuel combustion were included for context, though considered coincidental rather than directly climate-driven. Jacobson's temperature-based estimates were incorporated, (Jacobson, 2008).

2.8 Mortality-Emissions Metric

For each scenario, cumulative climate deaths (starvation/conflict, disasters, air pollution) were estimated from 1900 to 2200. These were divided by cumulative CO_2 emissions to produce a deaths-per-megatonne metric. Because deaths reduce to zero as atmospheric CO_2 concentration drops to 350 ppm and emissions drop to zero according to the different zero emission scenarios, cumulative deaths and cumulative emissions both eventually reach asymptotic values. The ratio of these represents the enduring human cost of fossil fuel emissions – cumulative lives lost per cumulative emission since 1900.

2.9 Potential Confounding Factors

Correlation does not prove causality, it only demonstrates the possibility of causation. Because multiple interacting drivers influence mortality outcomes, the analysis focuses on identifying broad empirical associations that are consistent with established physical and socioeconomic climate mechanisms, while explicitly recognising substantial uncertainty and potential confounding. Across such a broad ranging study there are a number of potential confounding factors that may simultaneously correlate with atmospheric CO_2 concentration and the mortality data. Table 1 describes the possible confounders identified, their effect and how they are considered or accepted as limitations of this study for further evaluation.

Table 1 Identified Potential Confounding Factors

Confounder	Effect	How Considered
Population growth	More people exposed	Undernourishment & conflict data is per capita data, the disaster data were tested for population normalisation
Population distribution / urbanisation	More people living in floodplains, coastal zones, informal settlements, fire-prone margins.	Not addressed to-date
Disaster reporting quality	EM-DAT reporting improves over time, especially after 1960–1980.	Disaster class modelling is dominated by post-1960 data.
Media / communications / state capacity	More disasters are detected and recorded now than in 1900.	Not addressed to-date
Disaster preparedness	Warning systems, evacuation, building codes, cyclone shelters reduce deaths per event.	Acts to mitigate mortalities, making our projections conservative
Healthcare improvements	Lower mortality from injury, disease, epidemics, famine complications.	Acts to mitigate mortalities, making our projections conservative
Agricultural technology	Fertilisers, irrigation, mechanisation, crop breeding, global trade can reduce undernourishment independent of climate.	Acts to mitigate undernourishment mortalities, making our projections conservative. These factors will affect both the prior to minimum and after minimum modelling.
Food trade / aid systems	International food imports and humanitarian aid decouple local crop failure from starvation.	Food aid did not appear to significantly affect undernourishment at regional scale (future publication).
GDP / poverty / inequality	Determines vulnerability to hunger, disaster mortality, displacement and conflict.	Methodology considers economic factors at Regional scale.
Conflict politics / governance	Civil war, state collapse, sanctions, military coups, ethnic violence can drive famine/conflict deaths independently of climate.	According to literature, undernourishment and conflict are inextricably linked – for this study, undernourishment and conflict deaths were combined and modelled together. Undernourishment overwhelmingly predominated.

Confounder	Effect	How Considered
Changing definitions / classification	What counts as “disaster”, “conflict death”, “undernourishment” may shift across datasets.	Consistent sources used for each cause. For health. The WHO datasets proved especially prone to this (ICD7 excluded). Only air pollution and heat/cold deaths were considered. Further work anticipated on climate associated health deaths.
Land-use change / deforestation	Affects floods, landslides, fires, crop productivity, and emissions.	Not addressed – if included in the trends and continues then forecast still pertinent.
Irrigation / groundwater depletion	Can mask climate impacts for decades, then fail abruptly.	Considered locally relevant but Regionally averaged out in trends estimated.
Globalisation / supply chains	Can buffer local shocks but also transmit food price crises globally.	Wealthier nations are insulated from climate vulnerability. Modelling considers this and how it might change if current economic trends continue.
Fertiliser and fossil-fuel inputs	Food production has risen partly because of fossil-fuel-dependent agriculture.	Not addressed – mitigating factor that makes our analysis conservative.
Adaptation	Air conditioning, sea walls, fire management, drought-resistant crops, migration.	Not addressed – mitigating factor that makes our analysis conservative.
Maladaptation / exposure growth	More assets and people built in hazardous areas can increase disaster losses independent of hazard change.	Not addressed

Overall, we believe that our efforts to mitigate confounding factors (especially population and economic factors at Regional scale) should have minimised mis-allocation. For the predominant undernourishment cause, the methodology should tend to cancel out somewhat the effect of confounding factors since the estimated mortalities comprise the difference between declining mortalities with time (proxy for development) and the increasing mortalities with CO2 concentration, where both are affected by any confounding factors.

2.9 Data Sources

All of the data used in this study are publicly available and their sources referenced as appropriate in the results sections.

2.9 Uncertainty

Confidence intervals (95%) were calculated for linearized regression-based categories. For starvation and conflict limited data results in very wide confidence limits. Limitations include the exclusion of emerging mortality pathways (unknown unknowns),

and the inability of historical data to inform the implications of accelerating compounding climate feedback loops.

The analysis seeks to be as comprehensive as possible but recognises that some categories overlap, data are incomplete or contested, and additional mortality pathways may emerge. Estimates are therefore contingent on available evidence and assumptions, so should be interpreted as indicative and precautionary rather than definitive especially when extrapolated far into the future. No broadly integrated global mortality framework currently exists for comparing the potential human implications of alternative emissions pathways.

3. Results

3.1 Results: Literature Survey

3.1.1 Climate-related mortality research

Climate-related mortality has been examined across several distinct domains:

- nutrition (UNICEF, 2023; UNICEF, 2021; FSIN, 2024; de Waal, 2018; Mirzabaev, Kerr et al, 2023; Myers, Zanobetti et al, 2014)
- conflict (Hsiang & Burke, 2014; Burke & Hsiang, 2015; Burke & Miguel, 2015; Schaar, 2018; Mobjörk,Gustafsson et al, 2016; Gleditsch, Wallensteen et al, 2002; Van Baalen & Mobjörk, 2018; World Bank, 2018; Conte & Migali, 2019; Petersen-Perlman,Veilleux et al, 2017),
- disasters (CRED, 2023; CRED, 2018), and
- health (Watts, Amann et al, 2018; World Health Organization, 2014; World Health Organization, 2023; World Health Organization, 2024; World Health Organization, 2025; Haines & Ebi, 2019; Black, Perin et al, 2000; MCC, 2025; Climate Impact Lab, 2025).

Individual pathways are well characterised for:

- heat exposure (World Health Organization, 2024; Gould, Heft-Neal et al, 2024; Zhao, Guo et al, 2021; Bressler, 2021; Carleton, Jina et al, 2022; Gasparrini, Guo et al, 2017; Dietz Gollier & Kessler, 2018)
- storm and floods (Knutson, Sirutis et al, 2015; United Nations, 2023)
- vector-borne disease (CDC, 2024))
- air pollution (Jacobson, 2008; World Health Organization, 2025),

However, there are few studies that attempt to integrate them into a single framework (Parncutt, 2019; Ciscar, Rising et al, 2019). This absence of synthesis limits comparability and constrains global mortality estimation.

3.1.2 Undernourishment and famine

Undernourishment is widely recognised as the largest potential driver of climate-induced deaths (CRED, 2018; Anonymous, 2007; IPCC, 2021; Roser, Ritchie et al, 2019; Dattani, Spooner et al, 2023). Declines in staple crop yields, water stress, and soil degradation are expected to exacerbate chronic undernourishment (Mirzabaev, Kerr et al, 2023). Acute famines often arise when these stresses interact with political instability, producing mortality surges (FSIN, 2024; de Waal, 2018; Conte & Migali, 2019).

3.1.3 Conflict and displacement

The literature increasingly acknowledges links between climate stress and violent conflict (Hsiang & Burke, 2014; Burke, Hsiang et al, 2015; Burke & Miguel, 2015; Schaar, 2018; Mobjörk, Gustafsson et al, 2016). While climate is rarely the sole cause, it acts as a risk multiplier through resource scarcity, migration, and governance stress (Hsiang & Burke, 2014; Burke & Hsiang, 2015; Burke, Miguel et al, 2009; Schaar, 2018; Mobjörk, Gustafsson et al, 2016; Gleditsch,Wallensteen et al, 2002; Van Baalen & Mobjörk, 2018; World Bank, 2018; Conte & Migali, 2019; Petersen-Perlman,Veilleux, 2017). Resulting deaths arise both directly (battle-related) and indirectly (through undernourishment, displacement and disease). Mortality estimates and especially forecasts are highly uncertain.

3.1.4 Extreme events and disasters

Extensive work has documented mortality from storms, droughts, floods, and wildfires (CRED, 2023; CRED, 2018; United Nations, 2023; IPCC, 2022). Improved warning systems and resilience have reduced per-event deaths in many regions (Delforge, Wathelet et al, 2023), but escalating hazard severity and exposure may reverse these trends (Parncutt, 2019; IPCC, 2022). Event attribution science now provides stronger evidence that many extreme events are intensified by anthropogenic warming (Ciscar, Rising et al, 2019; World, 2023; Ripple Wolf et al, 2023).

3.1.5 Health impacts

Health outcomes arise from both direct climate stress (heat, cold) and indirect undernourishment and disease (UNICEF, 2023; World Health Organization, 2024; Haines & Ebi, 2019; Black & Perin, 2000; World Health Organization, 2023; MCC, 2025; Climate Impact Lab, 2025; World Health Organization, 2024). Malaria and dengue expansion into higher altitudes, cholera sensitivity to warming seas, and cardiovascular deaths from heat waves are well established (UNICEF, 2023; Haines & Ebi, 2019; Black, Perin et al, 2024; World Health Organization, 2024). Under-reporting in low-income settings continues to hinder accurate global estimates (Haines & Ebi, 2019; MCC, 2025). Of the 749 WHO medical conditions reported in the WHO database (WHO, 2024), only 88 showed even a tenuous climate correlation whilst 160 showed a tennuous inverse climate correlation. More work is needed on this tentative finding.

3.1.6 Integrated assessments

Few efforts synthesise all mortality categories. Disaster-focused studies provide partial estimates (CRED, 2023), while health-specific global burden models offer parallel but incomplete perspectives (Watts, Amann et al, 2018; World Health Organization, 2014; Haines & Ebi, 2019; Black & Perin, 2000; MCC, 2025; Climate Impact Lab, 2025; World Health Organization, 2024). Some attempts to link climate and conflict exist (Hsiang & Burke, 2014; Burke, Hsiang et al, 2015; Burke, Miguel et al, 2009; Schaar, 2018; Mobjörk Gustafsson et al, 2016; Gleditsch,Wallensteen et al, 2002; Van Baalen & Mobjörk, 2018; World Bank, 2018; Conte & Migali, 2019; Petersen-Perlman, Veilleux et al, 2017), but none integrate undernourishment, conflict, disasters, and health into a unified framework. This study addresses that gap, combining historical regression models with scenario-based projections.

3.2 Climate Data and Correlations

Global temperature trends, emissions growth, and population dynamics were analysed using datasets from NASA (NASA, 2022; Ritchie Rosado et al, 2023; United Nations, 2024). Emissions pathways were modelled under net zero by 2050, 2060, 2070, and BAU, with CO_2 concentrations estimated including drawdown (Moore & Braswell, 1994). Equations 1–6 and Figures 1–6 illustrate these pathways.

Fig. 1 Global Mean Surface Temperature Anomaly relative to 1850–1900.

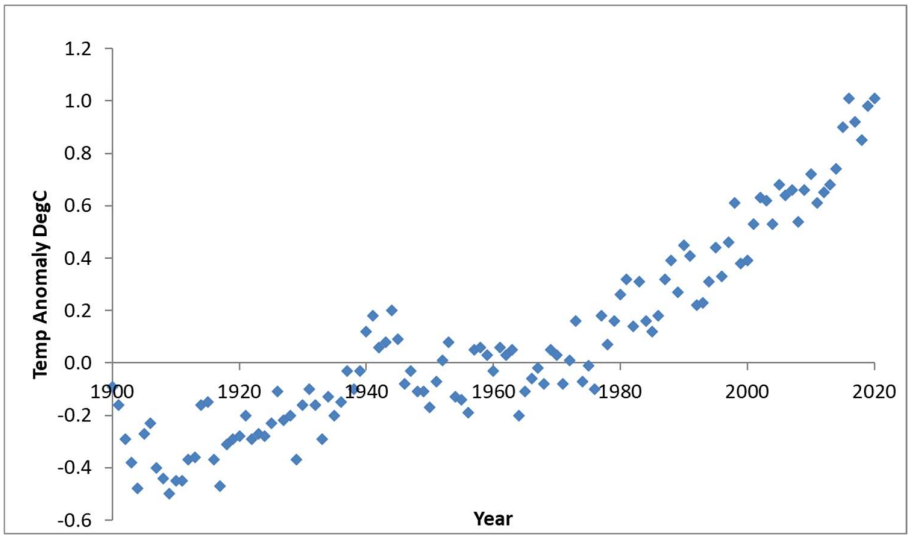

Source: NASA Vital Signs–Climate Change (NASA, 2022).

Global CO_2 emissions growth in Figure 2 shows that emissions have risen steeply since 1900 primarily due to fossil fuel combustion and land-related processes (Ritchie Rosado et al, 2023; Shukla, Skea et al, 2022).

Fig. 2 Global CO_2 emissions growth since 1900.

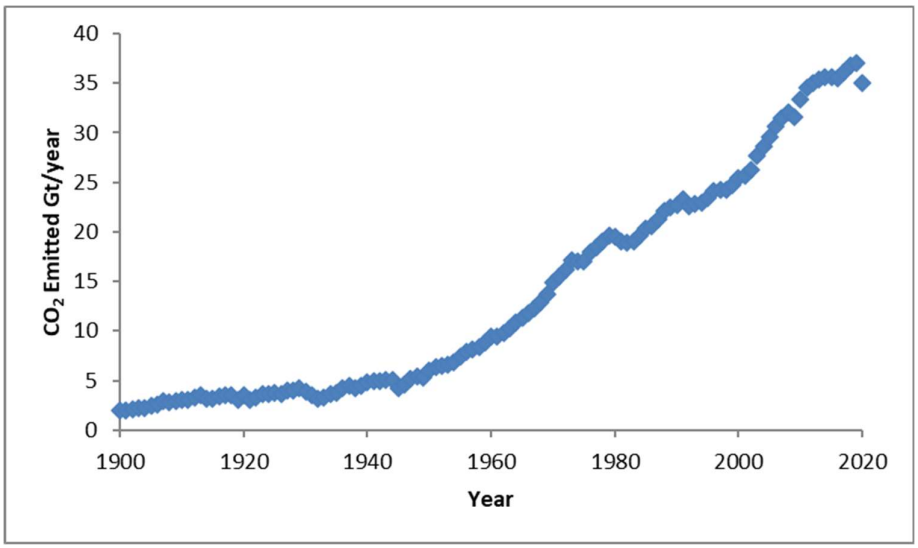

Source: Ritchie et al. (Ritchie, Rosado et al, 2023).

Historical and projected population growth is shown in Figure 3, with UN median forecasts implying stabilization by 2100 (United Nations, 2024). These projections are used in the modelling framework but are significantly altered when climate-related mortality is incorporated (see Section 4.7, Figure 17a).

Fig. 3 Historical and projected global population growth.

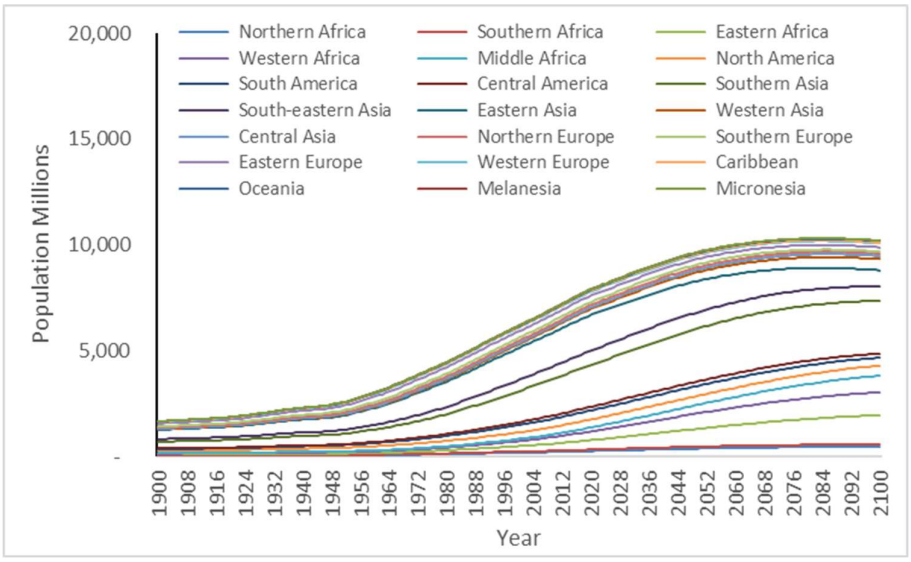

Source: UN World Population Prospects 2024 (United Nations, 2024).

Emissions appear closely correlated with population (Figure 4), though disproportionate contributions from wealthier groups are well documented.

Fig. 4 CO_2 emissions versus global population.

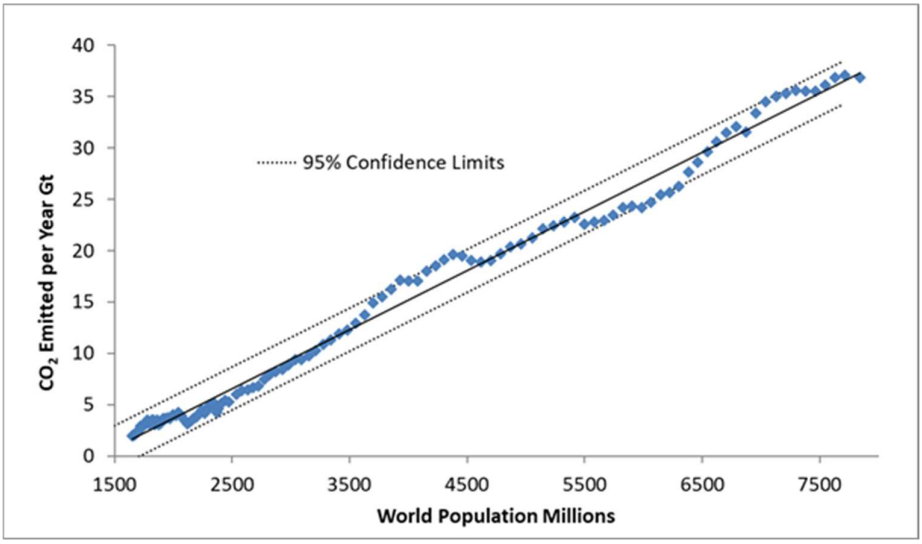

A regression model links population to annual emissions (Eq. 1):

CO_2 emitted$_{year}$ = 0.0057 x World Population Millions - 7.78 Gt equation 1
R^2 = 0.99 Standard Range = 1.05 Gt CO_2

Emissions scenarios. For future trajectories, emissions reductions are assumed to follow S-curve declines beginning in 2030, until the net zero year (by 2050, 2060, or 2070). The generic form (Eq. 2) applies, with parameters listed in Table 1.

CO_2 emitted$_{year}$ = exp (- S-curve factor * (y - 2030)) x CO_2 emitted$_{2030}$ Gt equation 2

S-Curve factors for the different scenarios are shown in Table 2:

Table 1. S-Curve factors Emissions Decline to Zero

Emissions decline from 2030	to 2050	to 2060	to 2070
S-curve factor	0.015	0.007	0.004

Atmospheric CO_2 concentrations reflect the cumulative emissions net of natural drawdown (via oceanic and terrestrial sinks). Assuming a composite atmospheric half-life of 72 years (Moore & Braswell, 1994), the concentration dynamics are represented by Eq. 3-5 and graphically in Figure 5.

CO_2 conc$_{year}$ = ((CO_2 conc$_{year-1}$ – CO_2 conc$_{preind}$)/ HLF) + CO_2 conc$_{preind}$ ppm equation 3

and the quantity of CO_2 removed each year is:

CO_2 removed$_{year}$ = (CO_2 conc $_{year-1}$ – CO_2 conc $_{year}$) /1000000 x MassAtmos Gt equation 4

Where:
CO_2 $conc_{preind}$ = 280 ppm (NASA, 2024)
Half Life = 72 years (Moore & Braswell, 1994)
Half-Life Factor (HLF) = exp(ln2/Half-Life) = 1.01 (exponential decay curve)
MassAtmosphere = 5.15 x 106 Gt (Lide, 2005)

CO_2 emitted, net natural $drawdown_{year}$ = CO_2 $emitted_{year}$ - CO_2 $removed_{year}$ Gt equation 5

Fig. 5 Projected atmospheric CO_2 concentrations under alternative mitigation scenarios (no climate deaths accounted).

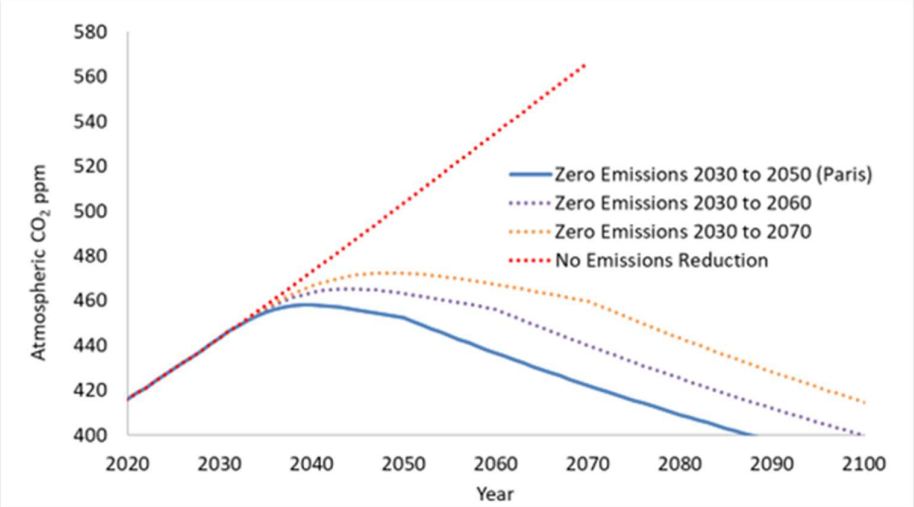

GMST is strongly correlated with net anthropogenic CO_2 (Figure 6, Eq. 6), consistent with the scientific consensus (IPCC, 2021).

GMST = 0.0009 x CO_2 emitted net natural drawdownyear + 13.8 DegC equation 6
R^2 = 0.894 Standard Range = 0.119 Deg.C

Fig. 6 GMST anomaly versus cumulative CO_2 emissions net of natural drawdown.

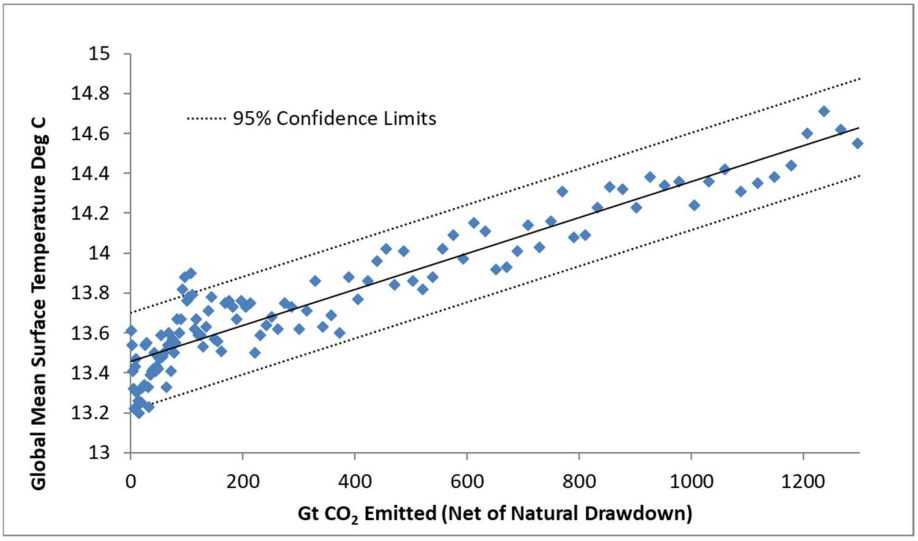

Each year's progression is modelled as:

For Each Year: Population → CO_2 Emissions → Net of Drawdown → Atmospheric CO_2 Concentration → Global Mean Surface Temperature Anomaly → Global Mean Surface Temperatures

3.3 Undernourishment and Conflict Deaths

Prior to 2010, global undernourishment declined substantially(Roser, Ritchie et al, 2019), broadly consistent with reductions in infant mortality (Dattani, Spooner et al, 2023) as many vulnerable low-income countries achieved modest development gains and rising GDP per capita. However, from around 2010—corresponding to atmospheric CO_2 levels of approximately 405 ppm—this trend reversed (Roser, Ritchie et al, 2019; Dattani, Spooner et al, 2023). Undernourishment increased despite continued improvements in infant survival, particularly evident across the most vulnerable regions and countries (Figure 7). This divergence is consistent with the possibility that climate-related pressures on agricultural productivity are beginning to offset some development-driven improvements in food security, a premise central to this study.

Conflict incidence (Our World in Data, 2023), has risen beyond historic ranges since 2000. However, conflict-related deaths show no clear trend, likely because the wide variability in fatalities per conflict obscures aggregate patterns.

Given the strong interlinkages between food insecurity, famine, and violence, undernourishment and battle deaths were combined for modelling purposes, though the estimates remain dominated by undernourishment-related mortality.

Fig. 7 Undernourishment Trend departing from Child Mortality Trend – World and Assorted Regions

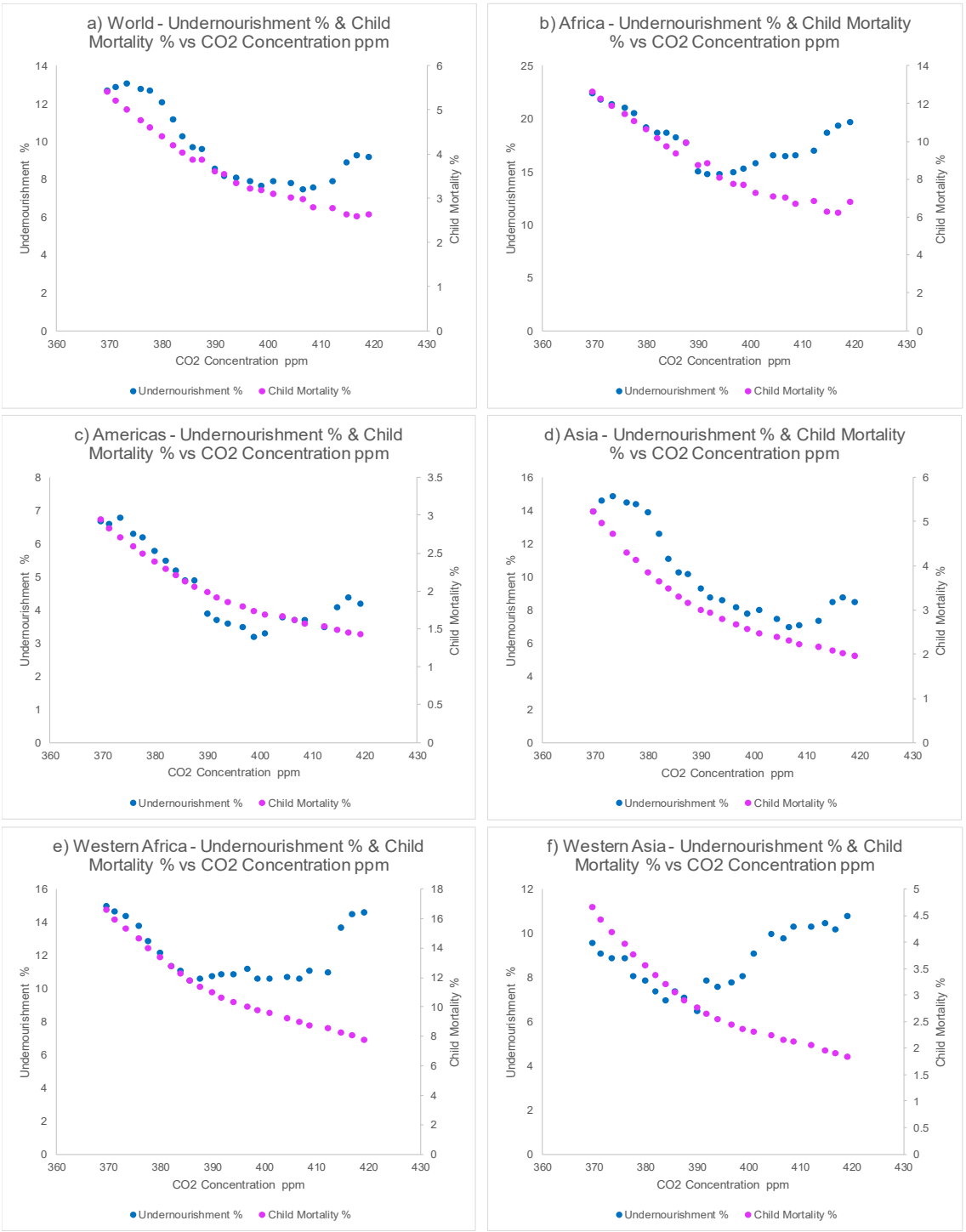

3.3.1 Global Modelling

The combined undernourishment and conflict world mortality data (Nf) were separated into two components using an iterative modelling process: a temporal decline function (Ny, Eq. 7) and a climate-driven component (Nc, Eq. 8). The temporal decline function assumes that the rate of decline increases with time (development/prosperity) but

decreases as the proportion of people still suffering undernourishment and conflict decreases. The climate driven function assumes that the rate of growth of those suffering undernourishment and conflict increases with CO_2 concentration, but then decreases as the proportion suffering approaches 100%.

The sum of these two functions should match the actual data observed (Nf) and at the point where the data changes from decreasing to increasing undernourishment and conflict, the two functions should be equal and equal half of the observed data. Successive iterations (Figure 8) separate the two functions if:

- at low CO_2 concentrations the decline function (Ny) approaches matching the actual data (Nf),
- at high CO_2 concentrations the climate driven function (Nc) approaches matching the actual data (Nf),
- at the swap over point both functions equal half of the actual data (Ny = Nc = Nf/2)

Beyond two iterations the results oscillated, so parameters were manually adjusted to optimise a least-squares fit to the actual data. The fitted curves suggest Ny may dominate below approximately 410 ppm of atmospheric CO_2 concentration and Nc emerging above 410 ppm of atmospheric CO_2 concentration (Figure 8b).

N_y (%) = exp(A . ln (y) + B) equation 7
R^2 = 0.98 Std. Range = 1.08% Pearson Coeff. = -0.99
Where y = year, A = -177, B = 1344

N_c (%) = 1 / (1 + exp(D . (C + E / D))) equation 8
R^2 = 0.96 Std. Range not reliably estimated from the limited data
Where C = Atmospheric CO_2 concentration (ppm), D = -0.0533, E = 29.39
[Note – E / D corresponds to the atmospheric CO_2 concentration where N_c = 50% - middle of the S-curve]

The combined results are shown in Figure 9, illustrating both the projected climate-driven mortality burden and the resulting impacts on global population size.

Fig. 8 Separating Undernourishment and Battle Deaths Decline with Time from Increases Probably due to Climate

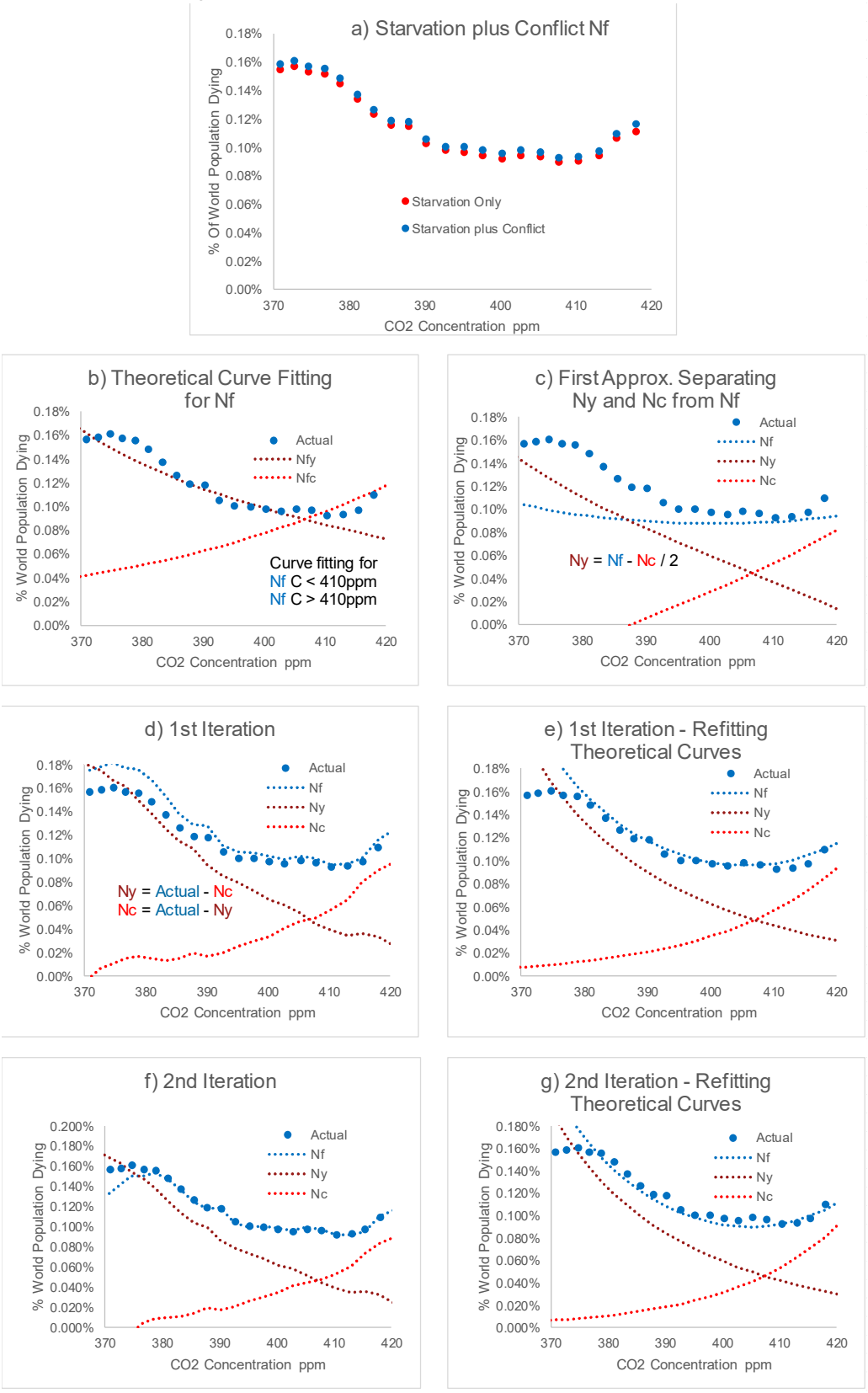

Fig. 9 Climate Related Deaths and Resulting Population Decline Global Modelling

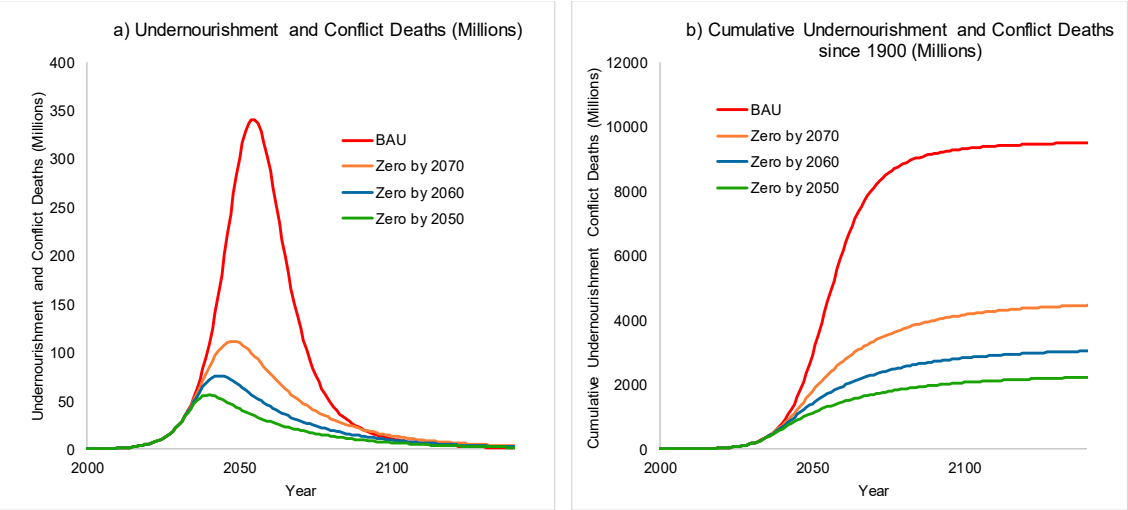

This results in forecast climate deaths from undernourishment and conflict as in Figure 9, with up to 300m deaths per year by mid 2050's for the BAU scenario and a collapse of global population from over 8bn to 600m by 2100. Zero emission scenarios show smaller deaths and sustain larger future populations. However, the global data to-date are dominated by regions where agriculture is most compromised by current, early levels of climate impact and where their populations are too poor to afford imported foods. For many regions, either climate change has yet to significantly affect agriculture or the population is wealthy enough to afford imported food and insulate people from undernourishment. A global estimate of mortality is therefore likely to over-estimate climate associated deaths by implicitly assuming uniform onset of climate-associated mortality for all – the forecast therefore needs regional granularity.

3.3.2 Regional Modelling

3.3.2.1 Climate Related Undernourishment

The methodology developed for the global data was repeated at a regional scale taking account of latitude (affecting the likelihood of climate impacts on agriculture) and economic factors affecting the proportion of populations economically vulnerable to undernourishment.

Undernourishment and conflict data were available for 22 regions which cover most of the global population. (Roser, Ritchie et al, 2019, Our World in Data, 2023). The regions were:

Eastern Africa	Middle Africa	Northern Africa	Southern Africa
Western Africa	Central America	North America	South America
Central Asia	Northern Asia	Southern Asia	Western Asia
Eastern Asia	South-eastern Asia	Caribbean	Eastern Europe
Northern Europe	Southern Europe	Western Europe	Melanesia
Micronesia	Oceania		

For a number of regions, levels of undernourishment were stable and very low (2.5% seems to be the minimum estimate) because these nations are economically protected from undernourishment and associated conflict. For these wealthy nations, there is no evidence of a decline in undernourishment with time so no basis for forecasting future vulnerability to climate change.

For poorer regions with apparent undernourishment and conflict causality, the coefficients A,B, D, E were obtained by iterating between the temporal decline function (equation 7) and the climate driven function (equation 8) and are shown in Table 2.

Table 2 Regional Factors ABDE for Modelling Undernourishment and Conflict Susceptibility to Climate (Equations 7 and 8)

Region	Ny - Factors					Nc - Factors					C50%
	A	B	R2	St.d Range	Pearson	D	E	R2	St.d Range	Pearson	ppm
Eastern Africa	-175	1324	0.91	0.11	-0.95	0.0300	-18.4	0.89	0.064	0.945	614
Middle Africa	-156	1182	0.79	0.14	-0.89	0.0251	-16.5	0.94	0.048	0.968	658
Northern Africa	-119	894	0.75	0.12	-0.86	0.0224	-16.8	0.83	0.076	0.909	750
Southern Africa	-89	671	0.57	0.07	-0.75	0.0290	-19.0	0.82	0.152	0.905	655
Western Africa	-191	1442	0.98	0.03	-0.99	0.0150	-13.1	0.89	0.048	0.942	870
Central America	No Data	No Data	No Data	No Data	No Data	0.0233	-16.3	0.80	0.092	0.892	698
North America	145	-1108	No Data	No Data	1.00	0.0382	-23.9	0.80	0.092	0.892	625
South America	-270	2049	0.96	0.13	-0.98	0.0596	-32.1	0.76	0.184	0.874	538
Central Asia	No Data	No Data	No Data	No Data	No Data	0.0355	-22.5	0.80	0.092	0.892	634
Northern Asia	-657	4985	1.00	No Data	-1.00	0.0432	-26.5	0.80	0.092	0.892	612
Southern Asia	-105	793	0.86	0.12	-0.93	0.0414	-24.1	0.98	0.024	0.989	582
Western Asia	-194	1466	0.94	0.08	-0.97	0.0351	-21.1	0.57	0.243	0.754	601
Eastern Asia	-351	2661	0.89	0.22	-0.94	0.0316	-20.5	0.80	0.092	0.892	649
South-eastern Asia	No Data	No Data	No Data	No Data	No Data	0.0226	-15.9	0.80	0.092	0.892	704
Caribbean	-100	757	0.81	0.11	-0.90	0.0266	-17.8	0.89	0.052	0.943	671
Eastern Europe	-348	2640	0.92	0.09	-0.96	0.0380	-23.8	0.80	0.092	0.892	626
Northern Europe	0	-9	No Data	No Data	No Data	0.0428	-26.2	0.80	0.092	0.892	613
Southern Europe	0	-9	No Data	No Data	No Data	0.0343	-21.9	0.80	0.092	0.892	638
Western Europe	0	-8	No Data	No Data	No Data	0.0378	-23.7	0.80	0.092	0.892	626
Melanesia	-50	376	0.55	0.10	-0.74	0.0120	-11.5	0.52	0.064	0.721	959
Micronesia	No Data	No Data	No Data	No Data	No Data	0.0195	-14.3	0.80	0.092	0.892	735
Oceania	-56	420	0.68	0.09	-0.82	0.0170	-14.8	0.74	0.056	0.859	867

The D,E factors for the climate related functions appear to vary approximately linearly with Latitude (Equations 9 and 10) but with a wide range of uncertainty (see Figure 10).

D Factor = 0.000427 x Latitude Deg + 0.0176 R^2 = 0.11 St.d Range = 0.009 Equation 9

E Factor = -0.219 x Latitude Deg -13.35 R^2 = 0.17 Std Range = 3.57 Equation 10

Fig. 10 Variation of D and E Factors with Latitude

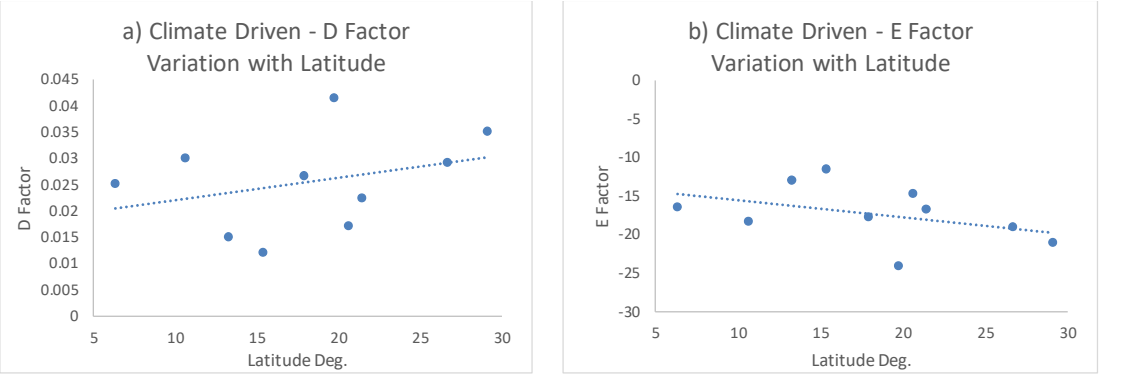

This gives us a tentative basis for estimating the climate vulnerability for regions whose potentially compromised agricultural productivity and undernourishment are currently masked by their wealth or latitude. The latitude estimated D and E factors in Table 2 are shaded grey.

There are many other factors influencing undernourishment sensitivity to climate reflected in the wide scatter of results and wide range of uncertainty. In the absence of a better basis, these factors are adopted for our modelling. It is assumed that averaged over the global scope these variations will mostly cancel for this approximate forecasting.

3.3.2.2 Wealth as a Mitigating Factor

Wealthy regions can afford to buy their way out of climate-associated food insecurity by importing food. This may allow some economically developing regions to alleviate current undernourishment as their prosperity increases. Equally some wealthy regions that may already have climate-compromised agriculture, may currently be economically protected from undernourishment but may be in slow economic decline compared to the global average as developing regions emerge economically. These currently wealthy regions may become vulnerable to undernourishment and economically emerging nations may become economically protected in the future.

Data were found for GDP/capita 2000-2023, for each of the 22 regions (Roser, Ritchie et al, 2019). On the assumption of compound economic growth, a growth factor was estimated for every region and globally (Table 3). Assuming the growth factors remain valid when extrapolated into the future, we can now approximately forecast GDP/capita for all regions.

Regions with growth factors exceeding the global value are regions that are getting relatively more prosperous in the world. If they are not suffering undernourishment, then they are likely to remain protected from undernourishment even if their agricultural productivity becomes compromised. If these regions are suffering undernourishment, then the growing prosperity of their people will allow them to progressively escape undernourishment.

Equally, regions with growth factors less than the global average are getting relatively less prosperous. If these regions are already wealthy enough to be protected from undernourishment, then into the future they will probably become increasingly vulnerable if their agriculture is, or becomes climate-compromised. If these nations are already suffering undernourishment then there is little prospect of them escaping and their levels of undernourishment are likely to get even worse.

Data were also found for median and poorest 10% of incomes 2000-2023 for each of the 22 regions (Eurostat, OECD, IMF, and World Bank, 2025). Assuming incomes are normally distributed (and that median is effectively the mean excluding outliers) the standard deviation of incomes can be estimated. Since we know the proportion of undernourished people in each region, we can estimate the income level that corresponds with each region's undernourished proportion and correlate this to GDP/capita for each region (Table 3).

If we know GDP/capita for each region (continuing the trend of compound growth/decline into the future relative to the global average), we can approximately forecast the proportion of each region's population with an income level low enough to make them vulnerable to undernourishment. For forecasting we assume that the income threshold for undernourishment inflates at the global compound interest rate, but each region's GDP/capita and hence daily incomes, inflates at the region's compound interest rate. In this way we account for regions economically shielding themselves or becoming economically vulnerable to undernourishment and conflict into the future.

Table 3 Regional Estimates of Compund Growth in GDP/capita and Daily Income Thresholds for Undernourishment

Region	GDP / cap Compound Growth Rate 2000-2023		Income threshold for undernourishment $/day 2000-2023	
	Mean	SD	Mean	SD
Eastern Africa	2.52%	1.71%	2.69	1.70
Middle Africa	0.88%	3.65%	2.92	0.94
Northern Africa	1.53%	1.73%	2.88	1.16
Southern Africa	0.97%	2.69%	2.17	0.54
Western Africa	2.11%	1.99%	2.02	0.54
Central America	2.25%	3.07%	4.03	0.59
North America	1.27%	1.80%	6.15	2.13
South America	1.64%	3.12%	3.98	0.74
Central Asia	4.39%	2.63%	3.60	0.73
Northern Asia	3.11%	4.06%	3.12	1.06
Southern Asia	4.31%	2.35%	3.05	0.82
Western Asia	2.02%	2.79%	6.44	2.55
Eastern Asia	5.26%	1.72%	11.65	3.86
South-eastern Asia	3.40%	2.41%	4.61	0.89
Caribbean	0.59%	3.03%	4.24	1.15
Eastern Europe	3.41%	3.16%	5.51	1.38
Northern Europe	1.21%	2.51%	14.22	2.29
Southern Europe	0.56%	3.33%	7.76	2.08
Western Europe	0.90%	2.20%	14.18	0.83
Melanesia	0.95%	3.37%	2.76	1.37
Micronesia	1.30%	2.55%	1.94	0.38
Oceania	1.32%	1.01%	7.58	5.38
World	0.00%	0.00%	0.00	0.00

3.3.3 Combining Climate Vulnerability and Wealth for Undernourishment

The proportions of regional population forecast to be suffering undernourishment can be estimated as the minimum of either the proportion that are vulnerable due to climate or the proportion likely to be vulnerable due to income. If the proportion climate vulnerable is less than the proportion income vulnerable, then climate vulnerability will be the determinant. If the proportion income vulnerable is less than the proportion climate vulnerable, then only those who lack the income to afford food will be vulnerable to undernourishment. In this way we are modelling the climate vulnerability and the economic vulnerability of regional populations complementarily.

For Each Year/Region: Year → Decline in Undernourishment and Conflict $\%_{Year, Region}$ (Exponential), Atmospheric CO_2 Concentration $_{Year}$ → Climate Related Vulnerability to Undernourishment and Conflict % Population $_{Year, Region}$.
GDP/capita compound growth/decline% $_{Year, Region}$ → Income Inequality $_{Year, Region}$ → Economically Vulnerable to Undernourishment and Conflict % Population $_{Year, Region}$.
Minimum [Climate Related Vulnerability to Undernourishment and Conflict $\%_{Year, Region}$ or Economically Vulnerable to Undernourishment and Conflict $\%_{Year, Region}$] x Population $_{Year-1}$ x Population Growth Factor $_{Year-1}$ – Climate Deaths $_{(Year-1)}$) → Undernourishment and Conflict Deaths $_{Year, Region}$.
Sum [Undernourishment and Conflict Deaths $_{Year, Region}]_{Regions}$ → Undernourishment and Conflict $Deaths_{Year}$

3.4 Deaths from Disasters

3.4.1 Trends in Disaster Frequency

Figure 10 shows the counts of disaster events since 1900, sourced from the EM-DAT database maintained by the Centre for Research on the Epidemiology of Disasters (CRED, 2023). Disasters such as fog, glacial lake outburst, impact events, and insect infestations were excluded due to limited data or no plausible link to climate forcing. Landslides (wet and dry) are combined into a single "mass movement" category (see Figure 10e).

EM-DAT defines a disaster as "an unforeseen and often sudden event which overwhelms local capacity… fulfilling at least one of the following: ten or more reported deaths, 100 or more persons affected, declaration of a state of emergency, or call for international assistance" (Centre, n.d.).

CRED warns of limitations in EM-DAT data, including inconsistent global coverage and possible biases stemming from variable reporting quality over time (Centre, n.d.). Despite these issues, EM-DAT remains a widely used and valuable global resource.

Figure 11 correlates disaster frequency with atmospheric CO_2 concentration, illustrating increasing occurrence in several categories. Table 2 (Results 3.6.2) summarizes the regression parameters per disaster class. Some categories (floods, landslides) show clear climate linkages; others (earthquake, volcanic) do not and are treated cautiously below.

3.4.2 Attribution: Climate vs. Exposure

To determine whether rising disaster counts reflect climate change or simply more people being exposed, events were normalized per million global population (Figure 12). This analysis suggests that increased counts of earthquakes and volcanic disasters are likely due to growing human exposure rather than climate, supporting their exclusion. By contrast, climate-sensitive categories continue to show rising incidence after normalization.

3.4.3 Severity: Deaths per Disaster

The fatalities per disaster vary widely (Figure 13), with extreme outliers complicating trend analysis. To reveal underlying patterns, high and low outliers were systematically excluded until the remaining dataset had a standard deviation approximately twice the mean. Table 3 details this cleaning process across disaster types.

The adjusted severity data (Figure 14) demonstrate varying trends:

- No climate-related trend: Deaths per disaster for earthquakes and volcanic eruptions show no consistent relationship with CO_2, reinforcing their exclusion.
- Subtle declines: Drought-related mortality per event slightly decreases over time—possibly due to better coping capacity or the general increase in precipitation extremes.
- Rising then plateauing: For floods, wildfires, mass movements, and epidemics, event severity increases with CO_2, but appears to plateau beyond ~370–390 ppm.

For forecasting, the long-term average severity (including historical outliers) is used, given that these distributions approximate log-normal behaviour (Results 4.6.2, Table 3).

Although the extreme variation in severity could reduce short-term predictive accuracy, long-term estimates should tend to converge toward the mean.

Fig. 11 Number of Disasters since 1900 (EMDAT)

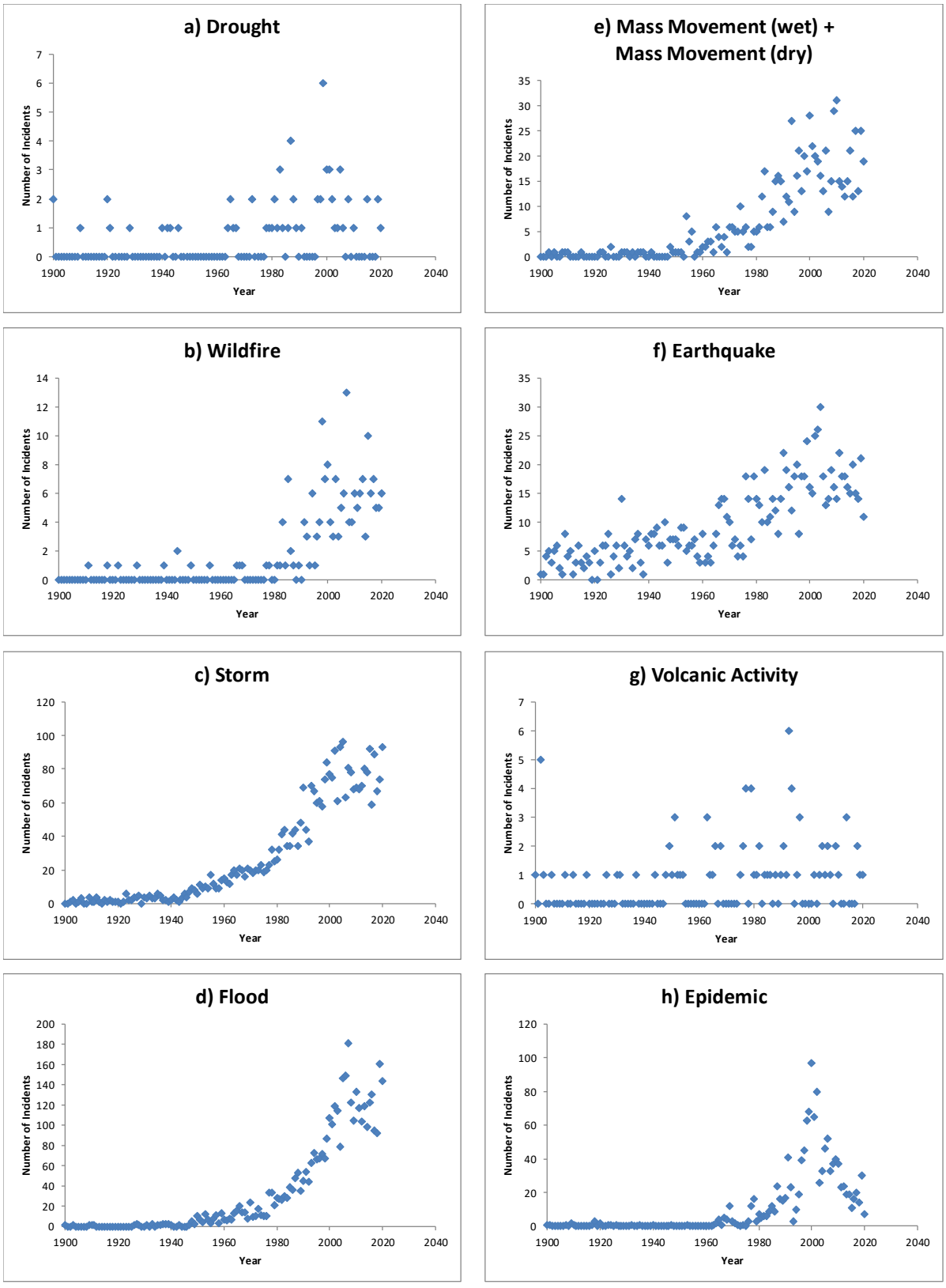

Fig. 12 Number of Disasters since 1900 (EMDAT) vs Atmospheric CO_2 Concentration

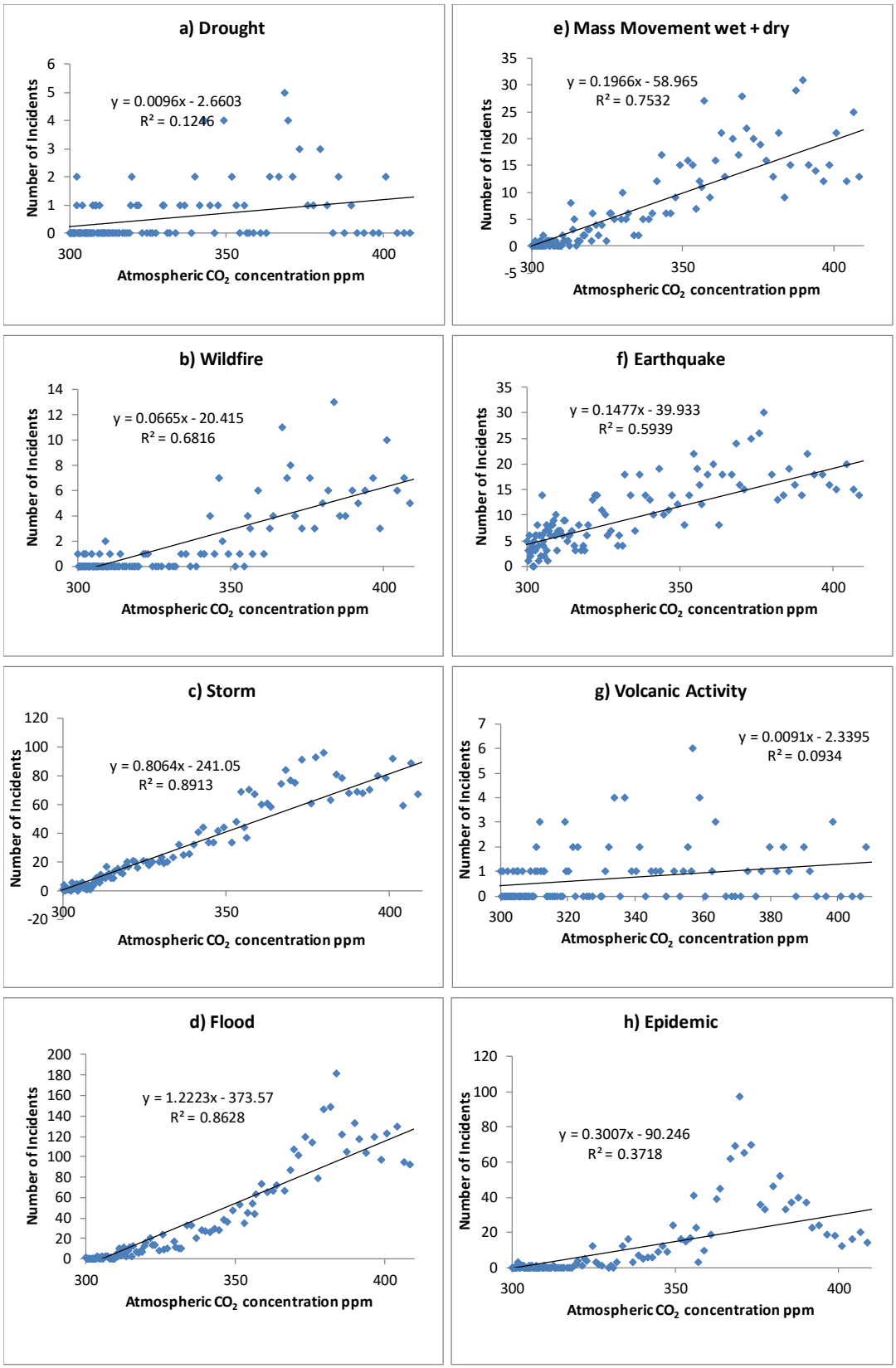

Fig. 13 Disasters (EMDAT) per Million Population vs Atmospheric CO_2 Concentration

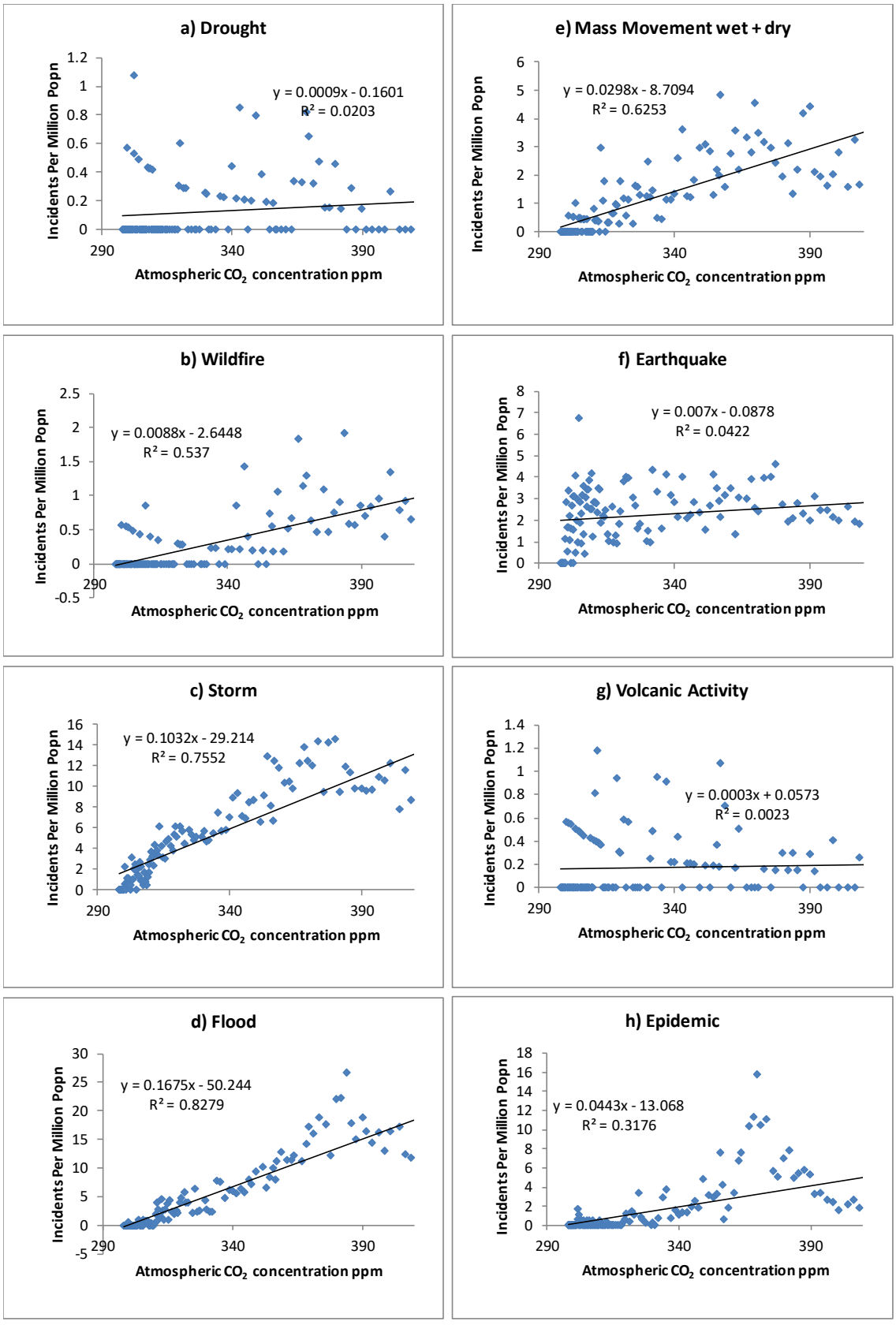

Fig. 14 EMDAT Data - Log Deaths per Disaster Histograms

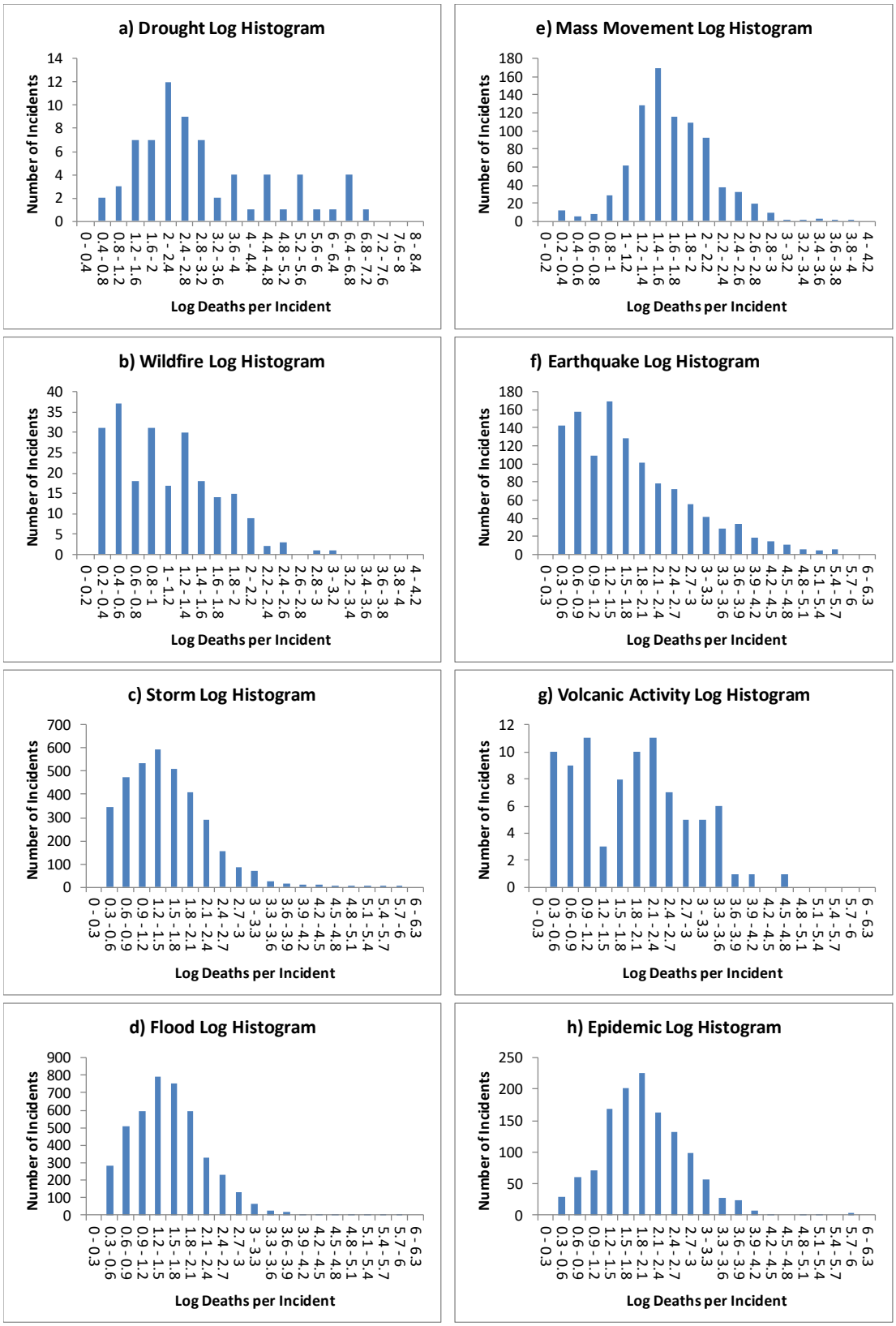

Fig. 15 Deaths per Million Population vs Atmospheric CO_2 (Excluding Outliers)

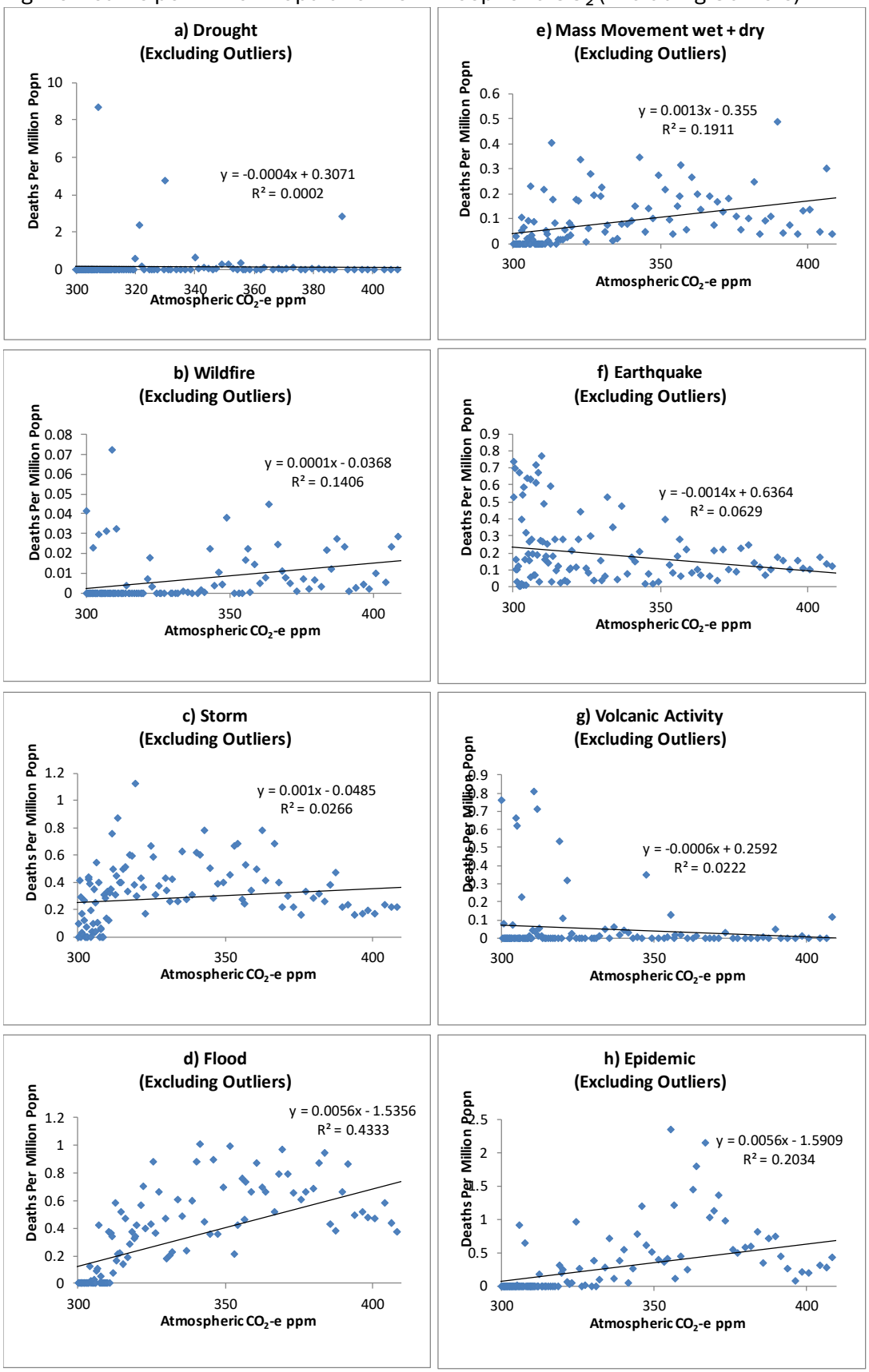

3.5 Health Deaths

3.5.1 Air Pollution Deaths

Whether air pollution mortality should be considered climate mortality may be arguable. However, if fossil fuel use is eliminated to mitigate climate change, associated air pollution deaths would also decline. According to the World Health Organization, approximately 7.39 million people died in 2019 from all forms of air pollution, including 3.23 million from indoor and the remainder from outdoor exposure (World Health Organization, 2025).

Jacobson estimates that ~90% of these deaths are energy-related and demonstrates a direct link between rising CO_2-equivalent concentrations and increased air pollution (Jacobson, 2008). His analysis suggests that ~20,000 additional air-pollution deaths occur annually for each 1 °C increase in global mean surface temperature (GMST). This effect arises because CO_2-driven chemical and meteorological changes increase ground-level ozone, particulates, and carcinogens.

Year-on-year GMST increases are used here to estimate added mortality (Eq. 9):

$\text{Air Pollution Deaths}_{year} = 20{,}000 \times (\text{GMST}_{year} - \text{GMST}_{preindustrial})$	Equation 9
Where $\text{GMST}_{preindustrial}$ = 13.7Deg C (NOAA average surface temperature 1850-1900)	

No uncertainty bounds are provided in Jacobson's study, so this relationship is applied at face value. Variation in GMST nonetheless provides a basis for estimating derived uncertainty.

3.5.2 Direct Temperature-Related Deaths

The most comprehensive global assessment of temperature-related mortality remains that of Zhao, Guo et al (2021). However, no suitable global incidence data were identified to generalise and extrapolate their findings by GMST or CO_2 concentration. Moreover, evidence and interpretation remain contested. Zhao et al nonetheless suggest that heat-related deaths could be significant, warranting future inclusion once suitable global datasets and greater consensus become available.

3.5.3 Other Health-Related Deaths

Broader health pathways remain uncertain and sometimes contradictory. A review of the WHO mortality database indicates that overall health-related deaths may decrease rather than increase with further warming.

Available data on diarrhoea (Black, Perin et al, 2024) and malaria (World Health Organization, 2023) do not reveal consistent correlations with either atmospheric CO_2 or GMST, despite WHO statements suggesting otherwise (refs needed here). These causes are therefore excluded from present forecasts. Ongoing work is investigating

correlations at the country level, where national mean temperatures and CO_2 trajectories may yield clearer signals.

3.6 Forecasting and Backcasting

Forecasting is used here to estimate climate-related deaths out to 2200, while backcasting distinguishes the historical climate related from non-climate related deaths since industrialisation (taken as 1900).

3.6.1 Starvation and Conflict

For starvation and conflict, the iterative equations developed in Section 3.2.3 (equation 1) are applied to both backcast mortality since 1900 and forecast deaths under future atmospheric CO_2 concentrations. This approach allows separation of the baseline decline in mortality due to development from the accelerating climate-induced increase after ~2010.

3.6.2 Disaster Deaths

For disasters, linear regression equations are used (Eq. 10), drawing on coefficients summarised in Table 4:

Disasters = Atmospheric CO_2 ppm x A + B	equation 10

Table 4. Disaster Numbers Regression Factors

Disaster Class	Slope A	Intercept B	R^2	Standard Range	Standard Range (from population forecast)
Drought	0.00964	-3	0.12	0.93	0.99
Wildfire	0.0665	-20	0.68	1.65	2.10
Storm	0.806	-241	0.89	10.2	15.7
Flood	1.22	-374	0.86	17.7	26.0
Mass Movement wet and dry	0.197	-59	0.75	4.09	5.42
Earthquake	0.148	-40	0.59	4.43	5.44
Volcanic activity	0.00911	-2	0.09	1.03	1.09
Epidemic	0.301	-90	0.37	14.2	16.2

Earthquake and Volcanic activity are excluded in future analysis as outlined in the above discussion.

The number of deaths per disaster is taken as the mean of the full sample (including outliers) as in Table 5:

Table 5 Deaths per Disaster Means and Standard Deviations

Disaster Class	Mean Deaths / Disaster	Standard Deviation Deaths / Disaster
Drought	150000	498000
Wildfire	24	77
Storm	390	6570
Flood	1600	64200
Mass Movement wet and dry	87	478
Earthquake	1920	14100
Volcanic activity	540	2390
Epidemic	5130	92330

While the short-term variability is extreme, long-term averages are assumed to approximate emerging trends. Earthquake and volcanic activity are excluded since they are unlikely to be climate driven.

3.6.3 Adjustments and Exclusions

Several adjustments are made to avoid double counting, lack of data or conflicting data:

- Drought deaths overlap with starvation; the lower estimate (drought) is excluded.
- Extreme temperature deaths are not included due to lack of reliable global datasets (see 4.5.2).
- Indirect pathways (crop failure, malnutrition, migration, conflict) are captured under the starvation/conflict model rather than disasters.

3.7 Total Forecast Climate Deaths and Cumulative Deaths per Cumulative Megatonne of CO_2 Emissions

The final results are summarised in Table 6 and shown graphically in Figures 15 and 16

Table 6 Summarised Forecasting and Backcasting Results to 2300

Metric		Scenarios			
			Zero Emissions by:		
		BAU	2070	2060	2050
Peak Climate Caused Deaths (Millions / year)	Low (yr)	Too Uncertain	8 (2043)	7 (2043)	6 (2039)
	Mean (yr)	Too Uncertain	24 (2033)	23 (2033)	23 (2033)
	High (yr)	Too Uncertain	92 (2043)	77 (2040)	62 (2037)
Cumulative Climate Caused Deaths (Millions) by 2300 since 1900	Low (yr)	**6122**	1114	984	865
	Mean (yr)	6150	1884	1704	1535
	High (yr)	**7893**	3767	3344	2923
Cumlative CO2 Emissions by 2300 since 1900 (Gt CO_2-e)	Low (yr)	8459	2210	2100	1990
	Mean (yr)	9063	2466	2356	2245
	High (yr)	7263	2715	2606	2497
Cumulative Climate Caused Deaths per Cumulative Mt of CO_2 emissions	Low (yr)	807	504	469	435
	Mean (yr)	820	764	723	683
	High (yr)	1277	1387	1283	1171

The business-as-usual results for climate deaths and cumulative deaths per cumulative megatonne of CO_2 emissions exhibit a surprising inversion between the Low and High forecast results. This appears to be due to the worst case of emissions growth causing such large numbers of climate-associated deaths out to ~2060, that even wealthy regions can succumb to undernourishment in the global competition for food.

In contrast, for the mean and low forecasts, the regions of Europe and South Asia that are currently wealthy enough to be insulated from food insecurity may experience declining prosperity by the 2100's exposing them to food insecurity, with significant consequences for climate deaths.

The higher early mortalities for the high range forecast reduce the global population significantly and therefore also reduce global emissions faster (emissions in this model are related to global population emitting) and hence reduce the climate forcing faster. In addition, there will be population growth for the climate survivors over this timescale. The result appears to be that the total number of deaths in the long-term is ironically greater for the Low and Medium forecasts than it is for the High forecast. Ironically, a slower onset of undernourishment through the 2000's may lead to greater mortality in the long-term. All of this only applies to the business-as-usual scenario. If mankind does actually achieve zero emissions somewhere close to 2050, then most of these deaths may be mitigated.

Fig. 16 Business As Usual Low, Mean, High Forecast Deaths per Year

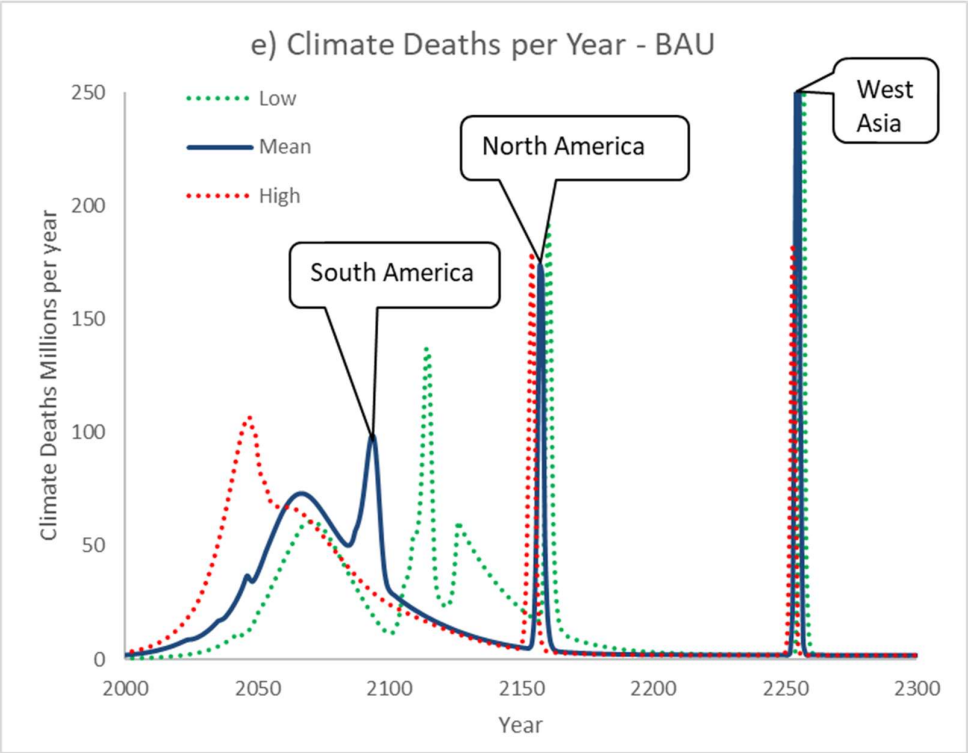

This model operates iteratively, with feedback loops linking climate-associated mortality, population, emissions, and atmospheric concentrations:

a) Rising climate-related deaths peak around 2040-2072, depending on the scenario except for economically-insulated regions (Figure 18 a & c; Table 6);
b) Rising mortality reduces the global population, especially for the BAU scenario (Figure 17a);
c) A smaller population reduces emissions from fossil fuel use (Figure 17b);
d) Slower emissions growth moderates the rise in atmospheric CO_2 (Figure 17c);
e) Natural drawdown processes (ocean uptake, photosynthesis, mineralisation) gradually reduces atmospheric concentrations (Figure 17d-f);
f) Lower atmospheric CO_2 concentrations, reduce temperature anomalies and stabilise global mean surface temperatures (Figures 17g–h);
g) Climate-related deaths decline as CO_2 and GMST reduce (Figure 18a)
h) Year-on-year climate-related deaths progressively reduce population, closing the loop (Figure 18a)
i) Population eventually stabilises at around 8.8bn if we do indeed get to net zero somewhere close to 2050. If we remain on the current trajectory, then BAU collapses global human population close to 5bn by 2150 (Figure 18a). Compounding climate feedback loops could make this far worse.

Figure 18b presents the cumulative climate deaths since 1900. Dividing these totals by the cumulative CO_2 emissions (Figure 17c) yields the metric of cumulative deaths per cumulative megatonne of CO_2 emissions (Figure 18f). Since both deaths and emissions

decline towards zero by ~2300, the ratio of cumulative deaths per cumulative megatonne converges to a single final value (Table 6).

Fig. 17 Climate Mortality Modelling – Population to Global Mean Surface Temperature

Fig. 18 Climate Mortality Modelling – Deaths per Year to Cumulative Deaths per Megatonne of CO_2-e

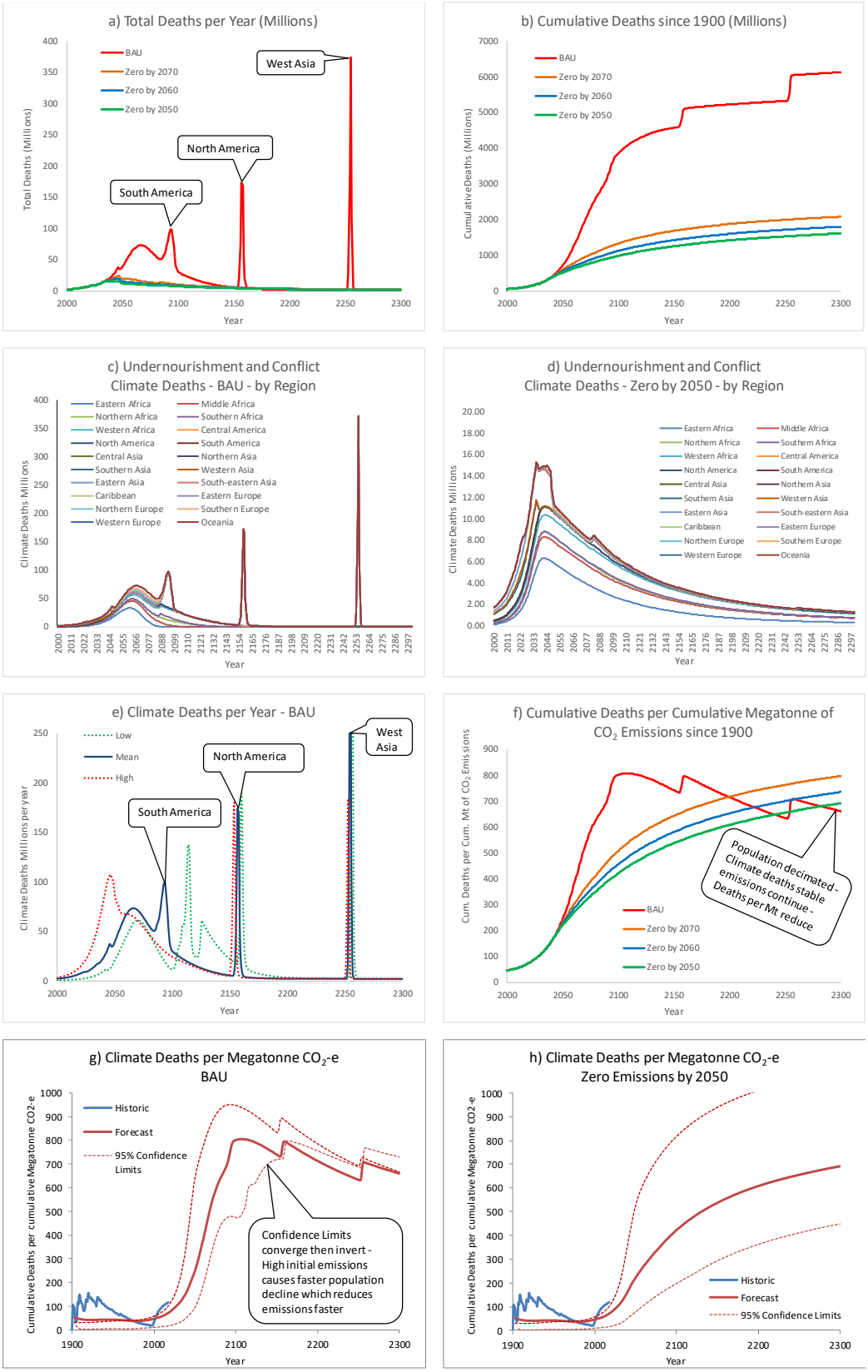

Figure 19 illustrates the relative contributions to climate deaths from the different causes for 2024 (a & b) 2050 (c & d) and 2200 (e &f). Undernourishment and conflict dominate the totals. Figures 19b, d and f exclude undernourishment and conflict to reveal the relative contributions of disasters, health impacts, and conflict to climate-related mortality.

Fig. 19 Causes of Climate Affected Deaths by 2024 and 2050

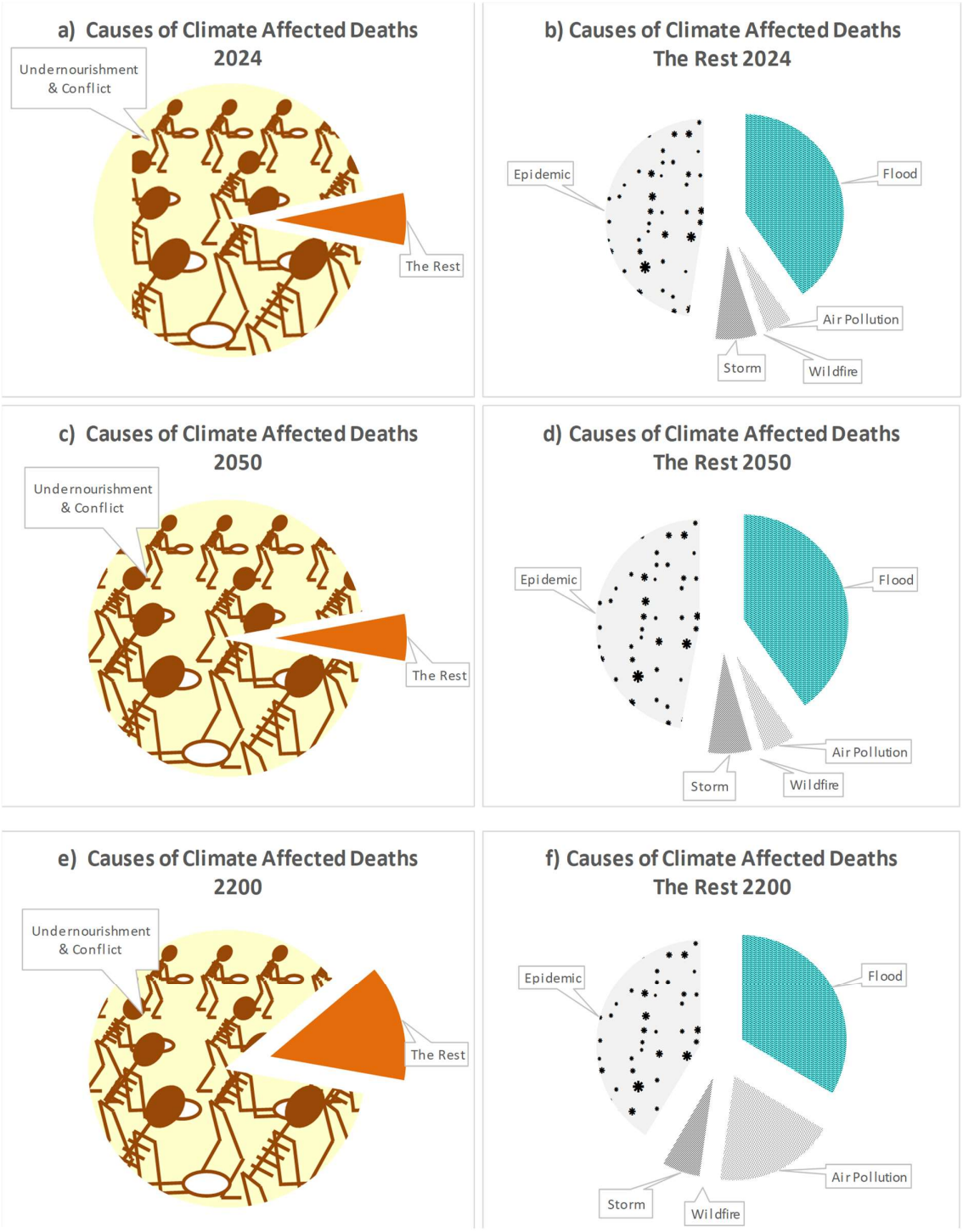

4. Conclusions

This study provides the basis for calculating the potentially catastrophic human consequences of failing to achieve net-zero greenhouse-gas emissions. Continuing on a business-as-usual (BAU) pathway of fossil-fuel combustion and rising emissions will lead to escalating mortality, with the burden falling predominantly on today's youth and the next generation. It also shows how to estimate mortality saved by increasing the levels of decarbonization.

Even under the Paris-aligned pathway of net zero by 2050, climate-related mortality is projected to peak at ~16 million deaths per year by ~2035 (Table 6). Under delayed mitigation (2060 or 2070), or BAU, the outcomes become increasingly severe, with risks of global population collapse if we remain on the current trajectory headed for 3^0C of warming.

This review demonstrates that climate change poses a large and foreseeable risk to human life that is insufficiently represented in prevailing policy appraisal frameworks. It also is not available to help net zero reporting systems to show how much climate-induced mortality can be saved.

Synthesising empirical evidence across multiple mortality pathways shows that cumulative emissions, rather than short-term damages, dominate long-term human outcomes. The proposed metric of cumulative climate deaths per cumulative Mt CO_2-e provides a transparent way to link emissions' decisions directly to expected loss of life, while remaining compatible with existing greenhouse gas accounting practices.

Although uncertainty is unavoidable, particularly in modelling conflict and starvation, this uncertainty strengthens rather than weakens the case for precautionary action. Under high-emissions trajectories, mortality risks escalate rapidly and disproportionately affect low-income and low-latitude populations that have contributed least to cumulative emissions. Conversely, rapid emissions reduction yields substantial and enduring benefits in lives protected.

The cumulative climate deaths per cumulative Mt CO_2-e (692, ranging from 448 to 1089 with 95% confidence) is more likely to be an underestimate but may be used to show mortality impacts as well as lives saved. Projects and policies can thus be assessed using this metric.. Companies and institutions can add these calculations to their certification and climate reporting.

These findings challenge the adequacy of purely monetary climate metrics and support the integration of explicit mortality considerations into climate policy, project assessment, and legal accountability. Recognising climate change as a major public health and ethical issue, not only an economic externality, is essential for informed decision-making.

List of abbreviations

- AGW Anthropogenic Global Warming
- BAU Business as Usual
- CO_2-e CO_2 equivalent
- CRED Centre for Research on the Epidemiology of Disasters
- DICE Dynamic Integrated Climate-Economy model
- EMDAT The International Disaster Database
- EU European Union
- GISS Goddard Institute for Space Studies
- GMST Global Mean Surface Temperature
- IAM Integrated Assessment Model
- IPCC Intergovernmental Panel on Climate Change
- MCC Mortality Cost of Carbon
- NASA National Aeronautics and Space Administration
- NOAA National Oceanic and Atmospheric Administration
- OWID Our World in Data
- SIDA Swedish International Development Cooperation Agency
- SPRI Social Policy Research Institute
- ppm parts per million
- UNEP United Nations Environment Programme
- WHO World Health Organisation

References

Anonymous. Death rates will rise because of global warming, researchers warn. ScienceDaily. (2007). Available from: https://www.sciencedaily.com/releases/2007/07/070702145431.htm

Black RE, Perin J, Yeung D, Rajeev T, Miller J, Elwood SE, et al. Estimated global and regional causes of deaths from diarrhoea in children younger than 5 years during 2000–21: a systematic review and Bayesian multinomial analysis. Lancet Glob Health. (2024);12(5):e1234-45. Available from: https://www.thelancet.com/journals/langlo/article/PIIS2214-109X(24)00078-0/fulltext

Bressler RD. The mortality cost of carbon. Nat Commun. (2021);12(1):4467.

Burger M, Tigre MA. Global Climate Litigation Report: (2023) Status Review. UNEP. 2023. Available from: https://www.unep.org/resources/report/global-climate-litigation-report-2020-status-review

Burke M, Hsiang SM, Miguel E. Climate and conflict. Annu Rev Econ. (2015);7(1):577-617. doi:10.1146/annurev-economics-080614-115430

Burke MB, Miguel E, Satyanath S, Dykema JA, Lobell DB. Warming increases the risk of civil war in Africa. Proc Natl Acad Sci U S A. (2009);106(49):20670-4. doi:10.1073/pnas.0907998106

Caney S. Climate change and the duties of the advantaged. In: Intergenerational Justice. Routledge; (2017). p. 321–46. https://www.researchgate.net/publication/346226629_Climate_change_and_the_duties_of_the_advantaged

Carleton T, Jina A, Delgado M, Greenstone M, Houser T, Hsiang S, et al. Valuing the global mortality consequences of climate change accounting for adaptation costs and benefits. Q J Econ. (2022);137(4):2037–105.

Centers for Disease Control and Prevention (CDC). Climate and health: vector-borne disease. Atlanta: CDC; (2024). Available from: https://www.cdc.gov/climate-health/php/effects/vectors.html

Centre for Research on the Epidemiology of Disasters (CRED). EM-DAT: The international disaster database, general definitions and concepts

Centre for Research on the Epidemiology of Disasters (CRED). EM-DAT: The international disaster database. 2023. Available from: https://www.emdat.be/

Chang C. The ‘extraordinary’ record-breaking data that has climate experts baffled. SBS News. (2024). Available from: https://www.sbs.com.au/news/article/daily-heat-records-keep-getting-broken-its-leaving-experts-baffled/x7h38zakp

Ciscar JC, Rising J, Kopp RE, Feyen L. Assessing future climate change impacts in the EU and the USA: insights and lessons from two continental-scale projects. Environ Res Lett. (2019);14(8):084010.

Climate Emergency Declaration. Climate emergency declarations in 2,359 jurisdictions and local governments cover 1 billion citizens. (2024). Available from: https://climateemergencydeclaration.org/climate-emergency-declarations-cover-15-million-citizens/

Climate Impact Lab. Climate Impact Lab, University of Chicago. (2025). Available from: https://impactlab.org/

Conte A, Migali S. The role of conflict and organized violence in international forced migration. Demographic Research. (2019);41:393-424. doi:10.4054/DemRes.2019.41.14

CRED. Natural disasters (2018). Technical report. Louvain: Institute of Health and Society, UC Louvain; 2018. Available from: https://www.cred.be/sites/default/files/CREDNaturalDisaster2018.pdf

Dattani S, Spooner F, Ritchie H, Roser M. Child mortality. Our World in Data. (2023). Available from: https://ourworldindata.org/child-mortality

de Waal A. Mass Starvation: The history and future of famine. Cambridge: Polity Press; (2018). xiv+260 p.

Delforge D, Wathelet V, Below R, Sofia CL, Tonnelier M, Loenhout JA, Speybroeck N. EM-DAT: the emergency events database. Research Square; (2023). doi:10.21203/rs.3.rs-3807553/v1

Dietz S, Gollier C, Kessler L. The climate beta. J Environ Econ Manag. (2018);87:258–74.

Erbach G. European climate law. Regulation (EU). (2021);1119(2021). Available from: https://climate.ec.europa.eu/eu-action/european-climate-law_en

Eurostat, OECD, IMF, and World Bank (2025) – with minor processing by Our World in Data. "GDP per capita – World Bank – In constant international-$" [dataset]. Eurostat, OECD, IMF, and World Bank, "World Development Indicators 122" [original data]. Retrieved from https://archive.ourworldindata.org/20251209-133038/grapher/gdp-per-capita-worldbank.html

FAO. Indicator 2.1.1 – Prevalence of undernourishment. (2025). Available from: https://dataexplorer.fao.org/

Fisher S, Snow D, Grant Z, M K. Peoples' climate vote. UNDP. (2021). Available from: https://www.undp.org/publications/peoples-climate-vote

Food Security Information Network (FSIN). Global Report on Food Crises (2024). Food Security Information Network; 2024. Available from: www.fsinplatform.org/grfc2024

Friedlingstein P, O'Sullivan M, Hauck J, Landschützer P, Le Quéré C, Luijkx IT, et al. Global carbon budget (2023). Earth Syst Sci Data. 2023;15(12):5301–69.

Gasparrini A, Guo Y, Sera F, Vicedo-Cabrera AM, Huber V, Tong S, et al. Projections of temperature-related excess mortality under climate change scenarios. Lancet Planet Health. (2017);1(9):e360–5.

Gingerich PD. Temporal scaling of carbon emission and accumulation rates: modern anthropogenic emissions compared to estimates of PETM onset accumulation. Paleoceanogr Paleoclimatol. (2019);34(3):329–35. https://agupubs.onlinelibrary.wiley.com/doi/full/10.1029/2018PA003379

Gleditsch NP, Wallensteen P, Eriksson M, Sollenberg M, Strand H. Armed conflict (1946)–2001: a new dataset. J Peace Res. 2002;39(5):615–37.

Gould CF, Heft-Neal S, Heaney AK, Bendavid E, Callahan CW, Kiang M, et al. Temperature extremes impact mortality and morbidity differently. NBER Working Paper No. 32195. (2024). Available from: https://www.scientificamerican.com/article/global-warming-and-health/

Haines A, Ebi K. The imperative for climate action to protect health. N Engl J Med. (2019);380(3):263-73. doi:10.1056/NEJMsr1807873

Hsiang SM, Burke M. Climate, conflict, and social stability: what does the evidence say? Climatic Change. (2014);123:39-55. doi:10.1007/s10584-013-0868-3

Hultgren, A., Carleton, T., Delgado, M. *et al.* Impacts of climate change on global agriculture accounting for adaptation. *Nature* **642**, 644–652 (2025). https://doi.org/10.1038/s41586-025-09085-w.

IPCC). Climate change (2021): The physical science basis. Contribution of Working Group I to the Sixth Assessment Report. Cambridge: Cambridge University Press; 2021.

IPCC. Climate Change (2022): Impacts, Adaptation, and Vulnerability. Contribution of Working Group II to the Sixth Assessment Report of the Intergovernmental Panel on Climate Change. Cambridge: Cambridge University Press; 2022. doi:10.1017/9781009325844

Jacobson MZ. On the causal link between carbon dioxide and air pollution mortality. Geophys Res Lett. (2008);35(3):L03809. Available from: https://www.researchgate.net/publication/241062753_On_the_causal_link_between_carbon_dioxide_and_air_pollution_mortality

Knutson TR, Sirutis JJ, Zhao M, Tuleya RE, Bender M, Vecchi GA, et al. Global projections of intense tropical cyclone activity for the late twenty-first century from dynamical downscaling of CMIP5/RCP4.5 scenarios. J Clim. (2015);28(18):7203–24.

Kravchenko S. Right to carbon or right to life: human rights approaches to climate change. Vt J Envtl L. (2007);9:513. https://www.researchgate.net/publication/228177060

Le Quéré C, Andrew RM, Friedlingstein P, Sitch S, Hauck J, Pongratz J, et al. Global carbon budget (2018). Earth Syst Sci Data. 2018;10(4):2141–94. https://essd.copernicus.org/articles/10/2141/2018/

Lide DR, editor. CRC Handbook of Chemistry and Physics. Internet Version (2005). Boca Raton, FL: CRC Press; 2005. Available from: http://www.hbcpnetbase.com

MCC. MCC Collaborative Research Network. An international research program on the associations between environmental stressors, climate, and health. (2025). Available from: https://mccstudy.lshtm.ac.uk/

Mirzabaev A, Kerr RB, Hasegawa T, Pradhan P, Wreford A, von der Pahlen MCT, et al. Severe climate change risks to food security and nutrition. Clim Risk Manag. (2023);39:100473.

Mobjörk M, Gustafsson MT, Sonnsjö H, Van Baalen S, Dellmuth LM, Bremberg N. Climate-related security risks: Towards an integrated approach. SIPRI; (2016). Available from: https://www.sipri.org/publications/2016/climate-related-security-risks

Moore III B, Braswell BH. The lifetime of excess atmospheric carbon dioxide. Glob Biogeochem Cycles. (1994);8(1):23–38.

Myers SS, Zanobetti A, Kloog I, Huybers P, Leakey AD, Bloom AJ, et al. Increasing CO_2 threatens human nutrition. Nature. (2014);510(7503):139-42.

Nachmany M, Setzer J. Global trends in climate change legislation and litigation: (2018) snapshot. Grantham Research Institute on Climate Change and the Environment. 2018. Available from: https://www.lse.ac.uk/GranthamInstitute/wp-content/uploads/2018/04/Global-trends-in-climate-change-legislation-and-litigation-2018-snapshot-3.pdf

NASA. Global Climate Change, Vital Signs: Carbon Dioxide. (2024). Available from: https://climate.nasa.gov/vital-signs/carbon-dioxide/?intent=121

NASA. Vital Signs – Climate Change: Global Temperature. (2022). Available from: https://climate.nasa.gov/vital-signs/global-temperature/

Newman P, Net Zero Cities with Sustainability: A Practitioner's Approach, Edward Elgar, London, (2025).

Nolt J. How harmful are the average American's greenhouse gas emissions? Ethics Policy Environ. (2011);14(1):3–10. https://www.researchgate.net/publication/232862992

Our World in Data. Deaths in armed conflict, World 1989–2022. Uppsala Conflict Data Program. (2023). Available from: https://ourworldindata.org/grapher/deaths-in-armed-conflicts-by-type

Parncutt R. The human cost of anthropogenic global warming: semi-quantitative prediction and the 1,000-tonne rule. Front Psychol. (2019);10:2323.

Petersen-Perlman JD, Veilleux JC, Wolf AT. International water conflict and cooperation: challenges and opportunities. Water Int. (2017);42(2):105–20.

Ripple WJ, Wolf C, Gregg JW, Rockström J, Newsome TM, Law BE, et al. The (2023) state of the climate report: Entering uncharted territory. BioScience. 2023;73(12):841–50. https://www.researchgate.net/publication/374975790

Ripple WJ, Wolf C, Lenton TM, Gregg JW, Natali SM, Duffy PB, et al. Many risky feedback loops amplify the need for climate action. One Earth. (2023);6(2):86-91.

Ripple WJ, Wolf C, Newsome TM, Barnard P, Moomaw WR. World scientists' warning of a climate emergency. BioScience. (2020);70(1):8–100. https://doi.org/10.1093/biosci/biz088

Ritchie H, Rosado P, Roser M. Greenhouse gas emissions. Our World in Data. (2023). Available from: https://ourworldindata.org/grapher/annual-co-emissions-by-region

Roser M, Ritchie H. Hunger and undernourishment. Our World in Data. (2019). Available from: https://ourworldindata.org/hunger-and-undernourishment

Schaar J. The relationship between climate change and violent conflict. Working paper. Green Toolbox/Peace and Security Toolbox. Stockholm: Sida; (2018). Available from:

https://cdn.sida.se/app/uploads/2020/12/01105650/working-paper-climate-change-and-conflict.pdf

Shukla PR, Skea J, Slade R, Al Khourdajie A, van Diemen R, McCollum D, et al. Climate change (2022): Mitigation of climate change. Contribution of Working Group III to the Sixth Assessment Report of the Intergovernmental Panel on Climate Change. Cambridge: Cambridge University Press; 2022. https://doi.org/10.1017/9781009157926

Steffen W, Rockström J, Richardson K, Lenton TM, Folke C, Liverman D, et al. Trajectories of the Earth System in the Anthropocene. Proc Natl Acad Sci U S A. (2018);115(33):8252-9.

UNFCCC. Climate Plans Remain Insufficient. More Ambitious Action Needed Now. (2022). Available from: https://unfccc.int/news/climate-plans-remain-insufficient-more-ambitious-action-needed-now

UNFCCC. Paris Agreement to the United Nations Framework Convention on Climate Change. Dec. 12, (2015). Available from: https://unfccc.int/process-and-meetings/the-paris-agreement

UNICEF. The state of food security and nutrition in the world (2023). United Nations Children's Fund; 2023.

UNICEF. UNICEF Conceptual Framework on Maternal and Child Nutrition. New York: UNICEF; (2021).

United Nations General Assembly. Convention on the Rights of the Child. United Nations Treaty Series. (1989);1577(3):1–23. Available from: https://www.unicef.org.au/united-nations-convention-on-the-rights-of-the-child

United Nations World Food Programme. In world of wealth, 9 million people die every year from hunger, WFP chief tells food system summit. (2021). Available from: https://www.wfp.org/news/world-wealth-9-million-people-die-every-year-hunger-wfp-chief-tells-food-system-summit

United Nations. Climate change-induced sea-level rise direct threat to millions around world, Secretary-General tells Security Council. New York: UN; (2023).

UN Climate Summit. (2023, April 25). Comparing climate impacts at 1.5°C, 2°C, 3°C and 4°C. Available from: https://unclimatesummit.org/comparing-climate-impacts-at-1-5c-2c-3c-and-4c/.

UNDRR & CRED (2020). The Human Cost of Disasters: An Overview of the Last 20 Years (2000–2019). United Nations Office for Disaster Risk Reduction. https://www.undrr.org/publication/human-cost-disasters-overview-last-20-years-2000-2019

United Nations. United Nations Framework Convention on Climate Change. New York: United Nations; (1992). Available from: https://unfccc.int/resource/docs/convkp/conveng.pdf

United Nations. World Population Prospects (2024). Available from: https://population.un.org/wpp/graphs?loc=900&type=Probabilistic%20Projections&category=Population&subcategory=1_Total%20Population

Van Baalen S, Mobjörk M. Climate change and violent conflict in East Africa: Integrating qualitative and quantitative research to probe the mechanisms. Int Stud Rev. (2018);20(4):547-75.

Watts N, Amann M, Arnell N, Ayeb-Karlsson S, Belesova K, Berry H, et al. The (2018) report of the Lancet Countdown on health and climate change: shaping the health of nations for centuries to come. Lancet. 2018;392(10163):2479–514. https://www.thelancet.com/journals/lancet/article/PIIS0140-6736(18)32594-7

WHO. Climate Change Key Facts. Geneva: World Health Organization; (2023). Available from: https://www.who.int/news-room/fact-sheets/detail/climate-change-and-health

World Health Organization. (2024). *Mortality Database* [Database]. https://www.who.int/data/data-collection-tools/who-mortality-database

World Bank. Groundswell: Preparing for Internal Climate Migration. Washington, DC: World Bank; (2018). Available from: https://documents.worldbank.org/en/publication/documents-reports/documentdetail/846391522306665751/main-report

World Bank. World Development Indicators. Washington DC: The World Bank; (2024). Available from: http://data.worldbank.org/indicator/NY.GNP.PCAP.CD

World Health Organization. Heat and health. Geneva: WHO; (2024). Available from: https://www.who.int/news-room/fact-sheets/detail/climate-change-heat-and-health

World Health Organization. Quantitative risk assessment of the effects of climate change on selected causes of death, 2030s and 2050s. Geneva: WHO; (2014).

World Health Organization. The Global Health Observatory: ambient air pollution attributable deaths. Geneva: WHO; (2025). Available from: https://www.who.int/data/gho/data/indicators/indicator-details/GHO/ambient-air-pollution-attributable-deaths

World Health Organization. WHO Malaria Policy Advisory Group (MPAG) meeting report, 18–20 April (2023). Geneva: WHO; 2023. Available from: https://www.who.int/publications/i/item/9789240074385

World Meteorological Organization (WMO). Provisional state of the global climate (2023). Geneva: WMO; 2023.

Zhao Q, Guo Y, Ye T, Gasparrini A, Tong S, Overcenco A, et al. Global, regional, and national burden of mortality associated with non-optimal ambient temperatures from 2000 to 2019: a three-stage modelling study. Lancet Planet Health. (2021);5(7):e415–25.

Supplementary Information

This Supplementary Information supports the review paper 'Forecasting Lives Lost to Climate Change' submitted to Sustainable Earth Reviews. It consolidates and extends methodological derivations, regression formulations, and sensitivity analyses, with particular emphasis on undernourishment and conflict mortality pathways. Where relevant, material is adapted from a companion research paper with greater technical detail, and aligned for consistency of notation, assumptions, and interpretation.

S1. Overview of Supplementary Structure

Sections S2–S5 provide detailed methodological derivations and sensitivity analyses supporting the main text. These materials are peer-reviewable and are intended to provide transparency rather than introduce new claims.

S2. Methodological Detail Supporting Main Text

2.1 Extended Literature Review

Additional references on undernourishment–conflict linkages and climate attribution are summarised here. This includes studies on famine causation, migration pressures, conflict onset under climate stress, and humanitarian impacts. These support the core narrative but were too detailed for the main text.

A literature survey was conducted to identify the main mechanisms by which climate change contributes to human mortality, prior attempts to quantify deaths at the global scale, and areas of conflicting evidence (key findings below). Publicly available historic datasets (1900–present) were compiled from international agencies including FAO (FAO, 2025), WHO (WHO, 2023), World Bank (World Bank, 2024), UN (United Nations, 2024), and EM-DAT (CRED, 2023). These datasets provided the empirical basis for correlating climate drivers—principally atmospheric CO_2 concentrations and global mean surface temperature (GMST)—with observed mortality outcomes.

2.2 Scenario Framework

Future deaths were modelled under the four emissions scenarios:

- Net zero by 2050 (Paris-aligned),
- Net zero by 2060,
- Net zero by 2070, and
- Business-as-usual (BAU), assuming continued emissions growth.

Population projections were based on the 2024 UN forecasts (United Nations, 2024), adjusted annually for climate-related mortality. In the BAU scenario, population decline from climate impacts becomes the main mode for reducing emissions, whereas in the mitigation scenarios emissions are modelled with an S-curve emissions reduction trajectory close to zero at the corresponding date. Atmospheric CO_2 concentrations were estimated year-on-year, accounting for natural carbon drawdown (through ocean

dissolution, through photosynthesis and through mineralisation) with a composite half-life of ~72 years (Moore & Braswell, 1994).

2.3 Empirical Forecasting of Climate

Rather than relying on complex integrated assessment models, this study extrapolated empirical relationships from historical data. Linear regressions were developed linking:

- population (United Nations, 2024) to emissions (Ritchie, Rosado et al, 2023),
- cumulative CO_2 emissions (net of drawdown) to Atmospheric CO_2 Concentration (NASA, 2024) and
- Atmospheric CO_2 Concentration (Ritchie, Rosado et al, 2023) to temperature anomally and GMST (NASA, 2022).
- These relationships provided the basis for forecasting mortality through to 2200.

2.4 Undernourishment and Conflict Deaths

The World Food Programme (United Nations, 2021) estimated that in 2021, of the 740 million people suffering undernourishment, 9 million people (~1.2%), mostly children, died. This proportion was applied to the forecast undernourishment rates to estimate mortality. Undernourishment related deaths emerged as the dominant category of climate mortality, with conflict strongly intertwined.

Analysis of 149 socioeconomic indicators across 268 countries showed few valid correlations. Table S1 Summarizes the findings. Highlighting potential correlations, but all showed wide ranges of variability.

Statistics Seeking Correlation		By Country									
		vs Undernourished %					vs Battle Deaths				
		Slope	Intercept	RSQ	STEYX	Pearson	Slope	Intercept	RSQ	STEYX	Pearson
Year	year	-0.109	2014	0.0446	6.85	-0.211	0.000093	2007	0.00398	11.1	0.0631
Education	Adjusted net enrollment rate, primary (% of primary school age children)	-0.859	86.7	0.202	19.6	-0.449	0.0000255	73.5	0.000187	23.9	0.0137
	Adjusted net enrollment rate, primary, female (% of primary school age children)	-0.917	79.5	0.208	22	-0.457	-6.28E-05	64.5	0.000942	26.1	-0.0307
	Adjusted net enrollment rate, primary, male (% of primary school age children)	-0.747	86.2	0.192	18.9	-0.438	-6.66E-05	73.6	0.00139	22.8	-0.0372
	Adolescents out of school (% of lower secondary school age)	0.447	36.8	0.069	22.1	0.263	-4.48E-05	44	0.0011	24.3	-0.0332
	Adolescents out of school, female (% of female lower secondary school age)	0.552	43.1	0.099	24.1	0.315	-0.000065	51.7	0.00223	26.4	-0.0472
	Adolescents out of school, male (% of male lower secondary school age)	0.232	37.4	0.0221	22.3	0.149	-7.76E-05	41.8	0.00394	23.7	-0.0628
	Children out of school (% of primary school age)	0.894	12.4	0.213	19.7	0.461	-1.62E-05	26.6	0.0000749	24.4	-0.00866
	Children out of school, female (% of female primary school age)	0.993	19.3	0.238	22	0.488	0.0000499	35.2	0.000587	26.8	0.0242
	Children out of school, male (% of male primary school age)	0.805	13.2	0.219	18.8	0.468	0.0000611	26.6	0.00117	23.3	0.0342
	Children out of school, primary	15810	1156000	0.0037	2980000	0.0608	11.7	1528000	0.00267	2957000	0.0516
	Children out of school, primary, female	5518	948400	0.000796	2418000	0.0282	9.1	1075000	0.00286	2214000	0.0535
	Children out of school, primary, male	8191	493100	0.0114	945400	0.107	10.5	704900	0.016	1075000	0.127
	Compulsory education, duration (years)	-0.0258	8.09	0.0172	2.26	-0.131	0.0000102	7.86	0.00529	2.19	0.0727
Poverty	Adjusted net national income per capita (current US$)	-54.5	1889	0.0446	3152	-0.211	0.003	1068	0.0000693	2947	0.00833
	GDP per capita (constant 2015 US$)	-112	4357	0.0591	6151	-0.243	-0.00491	2619	0.0000494	5853	-0.00703
	GDP per capita (current US$)	-63.6	2423	0.0521	3717	-0.228	0.00101	1378	5.95E-06	3472	0.00244
	Population living in slums (% of urban population)	0.58	53.2	0.0857	22.3	0.293	0.0000265	59.1	0.000284	23.5	0.0169
	Poverty gap at $3.00 a day (2021 PPP) (%)	0.837	5.8	0.181	13.1	0.426	-0.00019	13	0.0127	14.1	-0.113
	Poverty gap at $4.20 a day (2021 PPP) (%)	1.25	10.4	0.246	16.1	0.496	-0.000286	21.2	0.017	18.3	-0.13
	Poverty gap at $8.30 a day (2021 PPP) (%)	1.84	24.8	0.295	21	0.543	-0.00035	40.4	0.0137	25	-0.117
	Poverty headcount ratio at $3.00 a day (2021 PPP) (% of population)	1.97	17.2	0.264	24.3	0.514	-0.000471	34.4	0.0193	28.3	-0.139
	Poverty headcount ratio at $4.20 a day (2021 PPP) (% of population)	2.46	26.7	0.306	27.3	0.553	-0.000547	47.8	0.0192	32.9	-0.138
	Poverty headcount ratio at $8.30 a day (2021 PPP) (% of population)	2.27	50	0.255	28.6	0.505	-0.000244	68.9	0.00388	32.8	-0.0623
Employment	Contributing family workers, total (% of total employment) (modeled ILO estimate)	0.19	21.5	0.0253	14.5	0.159	-1.42E-05	24.1	0.000112	14.7	-0.0106
	Contributing family workers, female (% of female employment) (modeled ILO estimate)	0.359	34.8	0.0331	23.8	0.182	0.0000943	39.4	0.00183	24	0.0428
	Contributing family workers, male (% of male employment) (modeled ILO estimate)	0.0941	14.8	0.0125	10.3	0.112	-1.06E-05	15.8	0.000133	10	-0.0116
	Employment in agriculture (% of total employment) (modeled ILO estimate)	0.472	44.4	0.0745	20.5	0.273	-8.91E-05	50.9	0.002	21.7	-0.0447
	Employment in agriculture, female (% of female employment) (modeled ILO estimate)	0.728	47.7	0.135	22.7	0.367	-3.58E-05	56.4	0.000259	24.3	-0.0161
	Employment in agriculture, male (% of male employment) (modeled ILO estimate)	0.321	44	0.0377	19.9	0.194	-6.99E-05	49	0.00129	21.2	-0.036
	Employment to population ratio, 15+, total (%) (national estimate)	-0.056	54.4	0.00135	10.9	-0.0367	-0.000103	54.1	0.00193	11.5	-0.044
	Employment to population ratio, 15+, female (%) (national estimate)	-0.757	41.1	0.0756	17.4	-0.275	-0.000305	36.3	0.0073	18.2	-0.0855
	Employment to population ratio, 15+, male (%) (national estimate)	0.736	68.4	0.242	8.8	0.492	0.0000108	73	0.0000262	10.7	0.00512
	Employment to population ratio, ages 15-24, total (%) (national estimate)	-0.192	46.5	0.0113	8.22	-0.106	0.00011	44.7	0.00272	9.18	0.0521
	Employment to population ratio, ages 15-24, female (%) (national estimate)	-0.663	40.7	0.0727	10.9	-0.27	0.000233	37.2	0.00803	11.3	0.0896
	Employment to population ratio, ages 15-24, male (%) (national estimate)	0.207	52.5	0.0156	7.54	0.125	-1.77E-06	52.2	6.89E-07	9.28	-0.00083
	Labor force participation rate for ages 15-24, total (%) (national estimate)	-0.0716	49.5	0.00258	10.7	-0.0508	-0.00011	49	0.00681	11.5	-0.0826
	Labor force participation rate for ages 15-24, female (%) (national estimate)	-0.615	40.6	0.0783	16	-0.28	3.47E-06	36	2.93E-06	17.7	0.00171
	Labor force participation rate for ages 15-24, male (%) (national estimate)	0.44	58.1	0.0864	10.9	0.294	-0.000214	61.6	0.0254	11.6	-0.159
	Labor force participation rate, total (% of total population ages 15-64) (modeled ILO estimate)	-0.23	67.5	0.0474	12.7	-0.218	-4.95E-05	65.3	0.0015	13.6	-0.0387
	Labor force participation rate, female (% of female population ages 15-64) (modeled ILO estimate)	-0.196	51.9	0.0105	23.6	-0.102	-9.68E-05	50.4	0.00182	24.1	-0.0426
	Labor force participation rate, male (% of male population ages 15-64) (modeled ILO estimate)	-0.253	82.6	0.162	7.09	-0.403	5.34E-06	79.9	0.0000514	7.92	0.00717
	Unemployment with basic education (% of total labor force with basic education)	-0.353	10.4	0.245	4.07	-0.495	0.000214	8.51	0.069	4.68	0.263
	Unemployment with basic education, female (% of female labor force with basic education)	-0.359	12.4	0.176	5.1	-0.419	0.000299	10.4	0.0936	5.54	0.306
	Unemployment with basic education, male (% of male labor force with basic education)	-0.384	10	0.297	3.88	-0.545	0.00018	8	0.0497	4.69	0.223
	Unemployment, youth total (% of total labor force ages 15-24) (national estimate)	-0.45	16.4	0.182	5.42	-0.427	0.000139	13.9	0.00556	6.04	0.0746
	Unemployment, youth female (% of female labor force ages 15-24) (national estimate)	-0.223	17.5	0.0197	8.95	-0.14	-0.00001	16.3	0.0000128	9.05	-0.00358
	Unemployment, youth male (% of male labor force ages 15-24) (national estimate)	-0.501	15.9	0.288	4.5	-0.534	0.000179	13	0.0111	5.47	0.105
Wealth Equality	Gini index	-0.108	39.3	0.00953	8.14	-0.0976	-0.000125	38.5	0.0176	7.87	-0.133
	Income share held by lowest 10%	0.036	2.5	0.0704	0.962	0.265	0.0000103	2.78	0.00794	0.968	0.0891
	Income share held by lowest 20%	0.0583	6.33	0.0449	1.98	0.212	0.000025	6.78	0.0114	1.96	0.107
	Income share held by second 20%	0.0266	10.7	0.00913	2.04	0.0955	0.0000306	10.9	0.0167	1.98	0.129
	Income share held by third 20%	-0.00385	15.2	0.000239	1.83	-0.0155	0.0000311	15.1	0.0219	1.75	0.148
	Income share held by fourth 20%	-0.0468	21.8	0.0626	1.33	-0.25	0.0000206	21.4	0.0168	1.32	0.13
	Income share held by highest 20%	-0.0318	46	0.00125	6.61	-0.0354	-0.000107	45.7	0.0198	6.35	-0.141
	Income share held by highest 10%	0.00854	30.3	0.000103	6.19	0.0102	-0.000103	30.4	0.021	5.92	-0.145
Population	Population	-437400	212200000	0.000244	383100000	-0.0156	-7083	185400000	0.00804	348600000	-0.0897
	Population density (people per sq. km of land area)	-0.938	115	0.014	109	-0.118	-0.000527	103	0.00177	106	-0.0421
	Population growth (annual %)	0.0133	2.03	0.0155	1.44	0.124	2.22E-06	2.28	0.000162	1.45	0.0127
	Rural population (% of total population)	0.47	56	0.106	18.6	0.325	-0.000045	64.6	0.000341	20.2	-0.0185
	Rural population growth (annual %)	0.0208	1.28	0.0305	1.6	0.175	0.0000073	1.65	0.00119	1.76	0.0345
	Rural population living in areas where elevation is below 5 meters (% of total population)	-0.026	1.32	0.06	1.35	-0.245	-9.31E-06	0.897	0.00897	1.35	-0.0947
	Urban population	-441700	47360000	0.00757	68890000	-0.087	-503	37880000	0.00414	64760000	-0.0644
	Urban population (% of total population)	-0.47	44	0.106	18.6	-0.325	0.000045	35.4	0.000341	20.2	0.0185
	Urban population growth (annual %)	0.0234	3.1	0.0318	1.76	0.178	-7.12E-06	3.64	0.00104	1.83	-0.0323
	Urban population living in areas where elevation is below 5 meters (% of total population)	-0.039	2.3	0.048	2.28	-0.219	-1.63E-05	1.65	0.0098	2.26	-0.099
	Death rate, crude (per 1,000 people)	0.147	10.6	0.0836	6.63	0.289	-9.4E-06	13.3	0.000102	7.71	-0.0101
Fertility	Fertility rate, total (births per woman)	0.0624	4.08	0.213	1.63	0.461	4.33E-06	5.13	0.000381	1.84	0.0195
	Birth rate, crude (per 1,000 people)	0.398	30.4	0.219	10.2	0.468	2.72E-07	36.8	3.94E-08	11.4	0.000198
	Adolescent fertility rate (births per 1,000 women ages 15-19)	1.28	83.6	0.111	49.2	0.333	-8.17E-05	104	0.000169	52.1	-0.013
Sex	Population, female (% of total population)	-0.00508	50	0.00301	1.26	-0.0549	0.0000104	49.9	0.00495	1.22	0.0704
	Population, male (% of total population)	0.00508	50	0.00301	1.26	0.0549	-1.04E-05	50.1	0.00495	1.22	-0.0704
	Sex ratio at birth (male births per female births)	-0.000292	1.06	0.0418	0.0191	-0.205	2.2E-08	1.05	0.0000955	0.0187	0.00977
Hygiene	People practicing open defecation (% of population)	0.481	22.5	0.0391	25.3	0.198	0.000111	25.7	0.00507	25.9	0.0712
	People using at least basic sanitation services (% of population)	-0.634	48.2	0.0507	29.1	-0.225	0.0000337	43.6	0.000362	29.6	0.019
	People using safely managed sanitation services (% of population)	-0.465	31.5	0.0465	22.9	-0.216	-0.000023	28	0.000374	23.2	-0.0193
Homicides	Intentional homicides (per 100,000 people)	-0.224	11.9	0.0106	15.6	-0.103	-5.59E-05	9.83	0.00112	15.2	-0.0335
	Intentional homicides, female (per 100,000 female)	-0.0798	6.3	0.00731	4.07	-0.0855	-2.15E-05	5.98	0.00677	4.15	-0.0823
	Intentional homicides, male (per 100,000 male)	0.761	33.8	0.00514	46.4	0.0717	-0.000361	36.9	0.0163	44.6	-0.128
Suicide	Suicide mortality rate (per 100,000 population)	-0.0115	7.03	0.000341	6.56	-0.0185	0.000093	6.93	0.0471	6.92	0.217
	Suicide mortality rate, female (per 100,000 female population)	0.0105	3.54	0.00128	3.07	0.0358	0.0000228	3.69	0.015	3.06	0.122
	Suicide mortality rate, male (per 100,000 male population)	-0.0388	10.7	0.00126	11.5	-0.0356	0.000174	10.3	0.0526	12.2	0.229
Political	Political Stability and Absence of Violence/Terrorism: Estimate	-0.0148	-1.3	0.0738	0.695	-0.272	-1.45E-05	-1.48	0.03	0.704	-0.173
	Political Stability and Absence of Violence/Terrorism: Percentile Rank	-0.159	13.9	0.037	10.7	-0.192	-0.000149	11.9	0.0138	10.8	-0.118
Representation	Voice and Accountability: Estimate	-0.0157	-0.528	0.0683	0.765	-0.261	-7.28E-06	-0.755	0.00631	0.783	-0.0794
	Voice and Accountability: Percentile Rank	-0.39	33.9	0.0613	20.2	-0.248	-0.000179	28.2	0.00543	20.7	-0.0737
Government	General government final consumption expenditure (% of GDP)	-0.0991	14.5	0.0382	5.37	-0.195	0.0000481	13.5	0.00292	5.72	0.0541
	Government Effectiveness: Estimate	-0.0241	-0.397	0.153	0.75	-0.391	-7.03E-06	-0.718	0.00569	0.796	-0.0755
	Government Effectiveness: Percentile Rank	-0.629	38.5	0.119	22.6	-0.346	-0.00023	30	0.00694	23.5	-0.0833
	Regulatory Quality: Estimate	-0.0228	-0.437	0.145	0.733	-0.38	-6.34E-06	-0.747	0.00485	0.778	-0.0697
	Regulatory Quality: Percentile Rank	-0.58	36.7	0.117	21.1	-0.341	-0.000207	28.5	0.00642	22.1	-0.0801
Military	Armed forces personnel (% of total labor force)	0.0529	1.87	0.0334	3.38	0.183	0.0000469	2.29	0.0246	3.23	0.157
	Battle-related deaths (number of people)	38	702	0.0592	1862	0.243	0.14	1579	0.0687	5446	0.262
	Military expenditure (% of GDP)	0.00878	3.15	0.00118	2.96	0.0343	0.0000267	3.56	0.00462	3.42	0.068
	Military expenditure (% of general government expenditure)	0.0464	10.7	0.00571	6.12	0.0755	0.0000937	12.1	0.0276	6.99	0.166
	Arms exports (SIPRI trend indicator values)	-1.06E+08	2.07E+09	0.0665	3.256E+09	-0.258	-13530	1.067E+09	0.00196	3.135E+09	-0.0443
	Arms imports (SIPRI trend indicator values)	2235000	583700000	0.000909	918400000	0.0302	-6744	586100000	0.00212	889700000	-0.0461
Corruption	Control of Corruption: Estimate	-0.0171	-0.592	0.127	0.593	-0.356	-2.93E-06	-0.804	0.0016	0.628	-0.0399
	Control of Corruption: Percentile Rank	-0.533	32.2	0.116	19.5	-0.341	-9.53E-05	25.6	0.00158	20.5	-0.0397
Law	Rule of Law: Estimate	-0.0232	-0.516	0.158	0.711	-0.397	-6.74E-06	-0.806	0.00568	0.763	-0.0754
	Rule of Law: Percentile Rank	-0.515	33.4	0.0944	21.1	-0.307	-0.000208	26.9	0.00653	21.9	-0.0808

Statistics Seeking Correlation		By Country									
		vs Undernourished %					vs Battle Deaths				
		Slope	Intercept	RSQ	STEYX	Pearson	Slope	Intercept	RSQ	STEYX	Pearson
Resources	Adjusted savings: natural resources depletion (% of GNI)	0.167	4.69	0.0417	10	0.204	0.000027	7.41	0.000463	10.1	0.0215
	Total natural resources rents (% of GDP)	0.105	8.6	0.0147	11.1	0.121	0.0000154	10.6	0.000134	11.3	0.0116
Energy	Adjusted savings: energy depletion (% of GNI)	-0.0118	3.2	0.00062	5.89	-0.0249	-7.68E-06	3.22	0.000104	6.03	-0.0102
	Fuel exports (% of merchandise exports)	-0.23	20.8	0.0063	30.9	-0.0794	-9.73E-05	18.7	0.000695	31.2	-0.0264
	Fuel imports (% of merchandise imports)	0.138	14.9	0.0155	11	0.125	0.0000868	15.6	0.00618	10.5	0.0786
	Oil rents (% of GDP)	-0.0425	5.38	0.00385	8.79	-0.0621	0.0000125	5.07	0.000129	9.53	0.0113
Minerals	Adjusted savings: mineral depletion (% of GNI)	-0.00152	0.166	0.00165	0.464	-0.0406	-1.66E-06	0.151	0.000631	0.523	-0.0251
	Ores and metals exports (% of merchandise exports)	0.121	4.43	0.0137	11	0.117	-2.36E-05	6.44	0.000345	12.1	-0.0186
	Ores and metals imports (% of merchandise imports)	0.0104	3.15	0.00295	1.9	0.0543	-1.02E-05	3.09	0.00269	1.88	-0.0519
	Mineral rents (% of GDP)	0.00183	0.297	0.000687	0.898	0.0262	-4.01E-06	0.334	0.00123	0.972	-0.035
Land	Surface area (sq. km)	-32420	2129000	0.0224	2942000	-0.15	-15.9	1611000	0.00215	2826000	-0.0464
	Land area (sq. km)	-18370	1648000	0.0136	2162000	-0.117	-14.2	1345000	0.00337	2077000	-0.058
	Rural land area (sq. km)	-16790	1411000	0.0117	2024000	-0.108	-2.28	1135000	0.000257	1959000	-0.016
	Urban land area (sq. km)	-267	17610	0.0146	28700	-0.121	-0.116	13020	0.00329	27870	-0.0574
	Agricultural land (sq. km)	-5462	634500	0.00877	798500	-0.0936	-4.63	538000	0.00258	749600	-0.0508
	Agricultural land (% of land area)	0.184	38.3	0.016	20	0.127	0.000227	40.9	0.009	20.2	0.0949
	Arable land (% of land area)	-0.208	23.5	0.027	17.3	-0.164	0.0000326	20.3	0.000251	17.4	0.0159
	Arable land (hectares per person)	-0.000516	0.303	0.00113	0.212	-0.0335	1.01E-06	0.286	0.00164	0.207	0.0406
Forest	Adjusted savings: net forest depletion (% of GNI)	0.171	1.57	0.0836	7.03	0.289	0.000033	4.28	0.00116	7.72	0.0341
	Forest area (% of land area)	-0.0387	24.3	0.000557	20.6	-0.0236	-0.000219	23.4	0.0139	20.1	-0.118
Agriculture	Permanent cropland (% of land area)	-0.0418	3.47	0.0192	4.12	-0.139	-1.76E-05	3.01	0.0012	4.3	-0.0347
	Land under cereal production (hectares)	-120200	19480000	0.00266	32180000	-0.0515	-212	17240000	0.00311	31770000	-0.0558
	Crop production index (2014-2016 = 100)	-0.000967	58.6	3.45E-07	22.7	-0.000587	0.000166	56.9	0.00359	23.5	0.0599
	Agricultural raw materials exports (% of merchandise exports)	0.0555	7.42	0.00192	13.6	0.0438	0.0000401	8.69	0.000775	13.7	0.0278
	Agricultural raw materials imports (% of merchandise imports)	0.0211	2.59	0.019	1.51	0.138	-1.65E-05	2.76	0.0093	1.62	-0.0964
	Agriculture, forestry, and fishing, value added (% of GDP)	0.479	20.2	0.193	11.2	0.44	-1.11E-05	28.1	0.0000548	13.9	-0.0074
Water	Level of water stress: freshwater withdrawal as a proportion of available freshwater resources	-0.794	63.3	0.0129	90	-0.114	0.000683	52.4	0.00315	85	0.0561
	People using at least basic drinking water services (% of population)	-0.502	66	0.0509	23	-0.226	-5.39E-05	61.4	0.00139	24.2	-0.0373
	People using safely managed drinking water services (% of population)	-0.685	39	0.0653	26.1	-0.255	0.0000221	34.8	0.000304	27.7	0.0174
Migration	International migrant stock (% of population)	-0.0497	3.71	0.0168	4.8	-0.129	-2.01E-05	3.14	0.00185	5.42	-0.043
	International migrant stock, total	-55790	3014000	0.04	3951000	-0.2	-24.2	1972000	0.0031	3798000	-0.0557
	Refugees under the mandate of the UNHCR by country or territory of origin	12760	80490	0.052	777700	0.228	5.97	259100	0.00551	757400	0.0742
	Refugees under the mandate of the UNHCR by country or territory of asylum	136	253600	0.0000092	608600	0.00303	-2.1	231400	0.00126	549900	-0.0355
	Refugees under the mandate of the UNRWA by country or territory of asylum	552	342900	0.0175	36380	0.132	-1.65	395000	0.0316	161900	-0.178
CO2 emissions	Carbon dioxide (CO2) emissions (total) excluding LULUCF (% change from 1990)	-1.35	43.3	0.0988	50.9	-0.314	-0.000235	35.5	0.00188	60.1	-0.0433
	Carbon dioxide (CO2) emissions excluding LULUCF per capita (t CO2e/capita)	-0.0862	3.26	0.0976	3.61	-0.312	0.0000128	1.84	0.000957	3.5	0.0309
Climate	Atmospheric CO2 Concentration ppm	-0.246	401	0.0442	15.6	-0.21	0.000203	386	0.00449	22.8	0.067
	Average Temperature Deg C	0.0896	20.8	0.0341	6.49	0.185	-5.62E-05	21.8	0.00419	6.53	-0.0648
Psychology	All - Narcissism	0.0175	3.86	0.158	0.28	0.398	-2.32E-06	3.96	0.00164	0.368	-0.0405
	All - Machaeavelianism	0.00573	2.9	0.00715	0.467	0.0845	5.43E-06	2.89	0.00579	0.457	0.0761
	All - Psychopathy	0.0388	2.5	0.277	0.434	0.526	-1.03E-06	2.83	0.000181	0.493	-0.0134
	Male - Narcissism	0.0213	4.07	0.204	0.291	0.452	2.05E-06	4.2	0.00112	0.394	0.0334
	Male - Machaeavelianism	0.00701	3.27	0.00871	0.517	0.0933	8.78E-06	3.27	0.0122	0.508	0.11
	Male - Psychopathy	0.0405	2.86	0.255	0.479	0.505	8.88E-07	3.21	0.000115	0.531	0.0107
	Female - Narcissism	0.0138	3.65	0.077	0.329	0.278	-6.7E-06	3.72	0.012	0.39	-0.11
	Female - Machaeavelianism	0.00445	2.52	0.00503	0.433	0.0709	2.09E-06	2.51	0.001	0.422	0.0317
	Female - Psychopathy	0.0372	2.14	0.258	0.436	0.508	-2.95E-06	2.46	0.00143	0.501	-0.0378
Aid	ODA Aid	-9.2	1232	0.0168	963	-0.13	0.00563	1057	0.00182	1017	0.0427
Undernourished	% Undernourished by Country	1	-	-	-	-	-1.28E-05	13.2	0.0000331	13.6	-0.00575
	Number Undernourished	491700	21970000	0.0112	63250000	0.106	-961	30350000	0.00604	63420000	-0.0777
	% of Undernourished World	6.26E-06	0.000337	0.00868	739	0.0932	-1.39E-08	0.000446	0.00607	0.000916	-0.0779
	Daily Calories per Capita	-14.9	2566	0.0562	950	-0.237	-0.00737	2375	0.00275	860	-0.0524

Deaths from undernourishment and battle deaths were combined for this modelling. A dual-empirical curve model was therefore developed to iteratively best fit the combined available undernourishment and battle deaths (see Results 5.3):

- A declining trend in undernourishment with time (Uy (%)), reflecting global development (improved nutrition, reduced poverty)
- An increasing trend in undernourishment linked to rising CO_2, representing the climate-driven impacts that we are attempting to determine.

For the global data, these opposing curves intersect around 2017, where the climate signal begins to outweigh development gains.

The global data on its own probably significantly overestimates undernourishment deaths because the data to-date is dominated by equatorial regions that are most vulnerable to current levels of warming and by poorer nations that cannot afford to import any short-fall in agricultural productivity exacerbated by climate change. It will not automatically be the case that continuing climate change will affect all regions equally for both of these reasons. Accordingly, for this study, the same iterative dual-empirical methodology was applied to the available regional undernourishment (and conflict) mortality data from 2000-2023.

This results in a set of regional factors (linearized S-curve gradient and intercept). These factors have then been linearly correlated with latitude (but with wide confidence limits), enabling an approximate model for the s-curve of climate caused undernourishment which was used for all regions where insufficient data was available for modeling or where the region has been economically insulated from climate caused undernourishment to-date. As climate change worstens, this provides the means to forecast approximately how additional regions are likely to become progressively exposed to climate caused undernourishment.

In addition, in wealthier regions, the population are wealthy enough to still afford food even though domestic production may be climate compromised, Poorer nations endure higher levels of undernourishment (see figures S1 and S2).

Figure S1 Undernourishment vs GDP/Capita

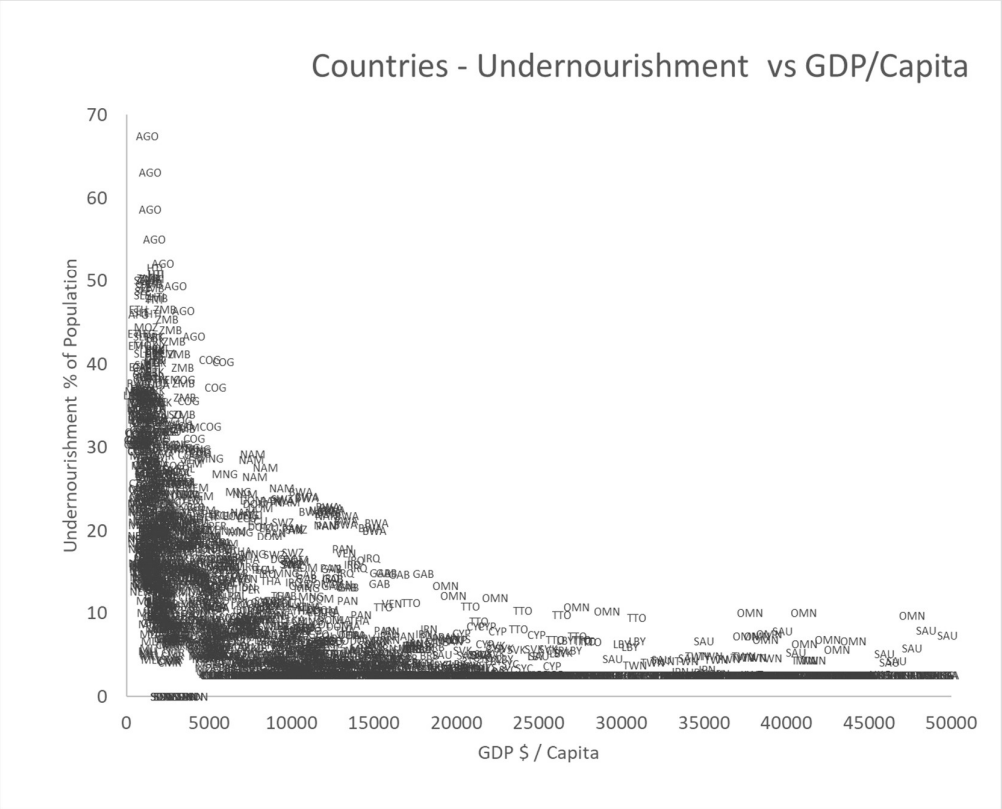

Figure S2 Undernourishment vs GDP/Capita - Histogram

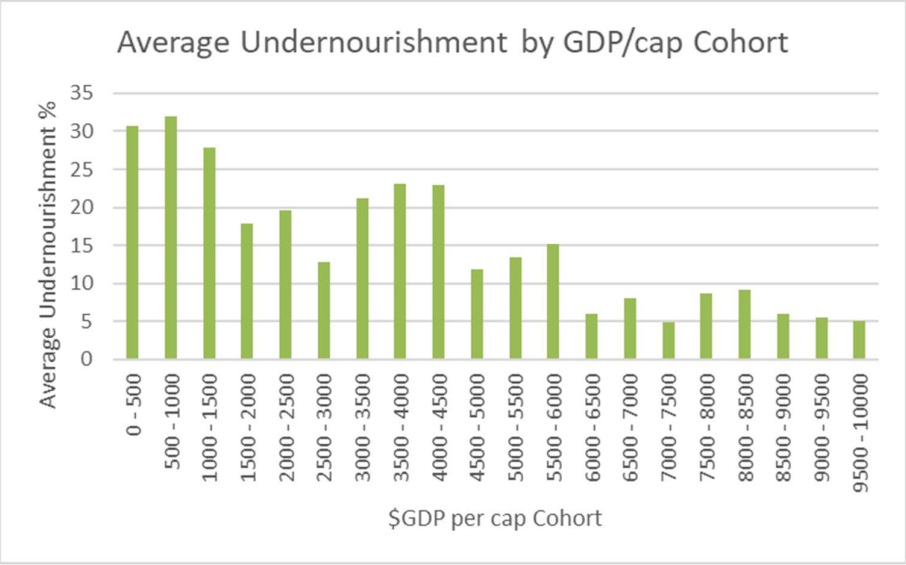

Global, regional and national data have been compiled for GDP/capita and the compound rate of growth (or decline) with time for all regions and times for which data

is available. Similar data have been compiled for the median and 10% poorest daily incomes. (Figure S3).

Figure S3 Median and 10% Poorest Daily Incomes. ($).

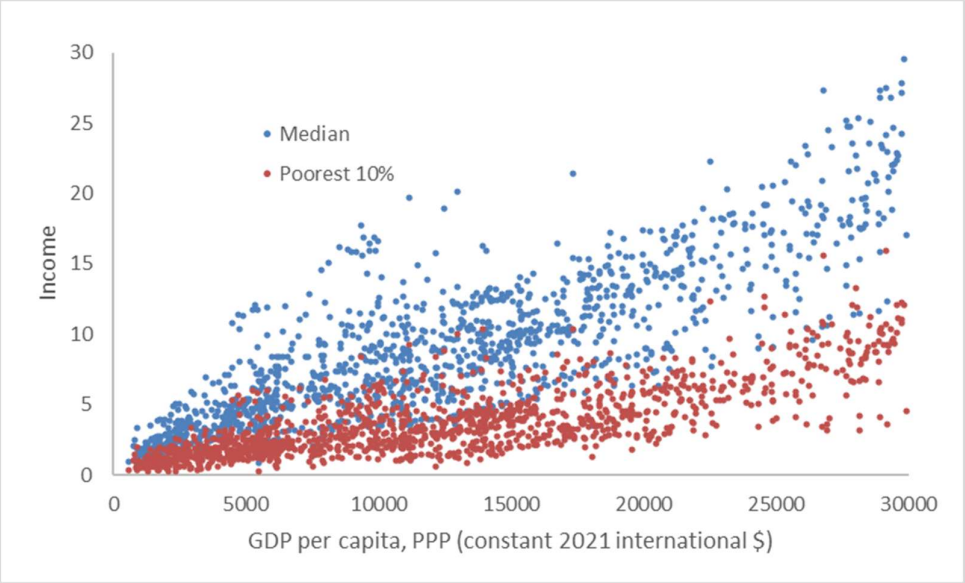

These data have been used to infer (assuming normally distributed) the standard deviation of incomes. (Figure S4) and their variation with GDP/Capita. Richer nations have a broader range of incomes!

Figure S4 Estimated Standard Deviation of Incomes

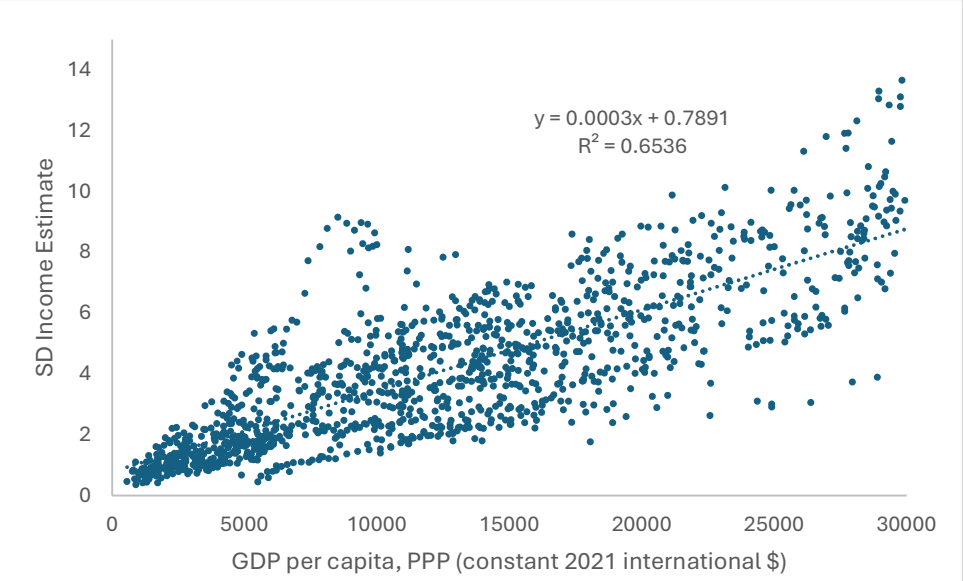

Since we know the proportion of undernourished people by region, we can now estimate the income level that corresponds to the same proportion of the population being undernourished.

Figure S5 Income ($ / day) Where % Poorer = % Undernourished

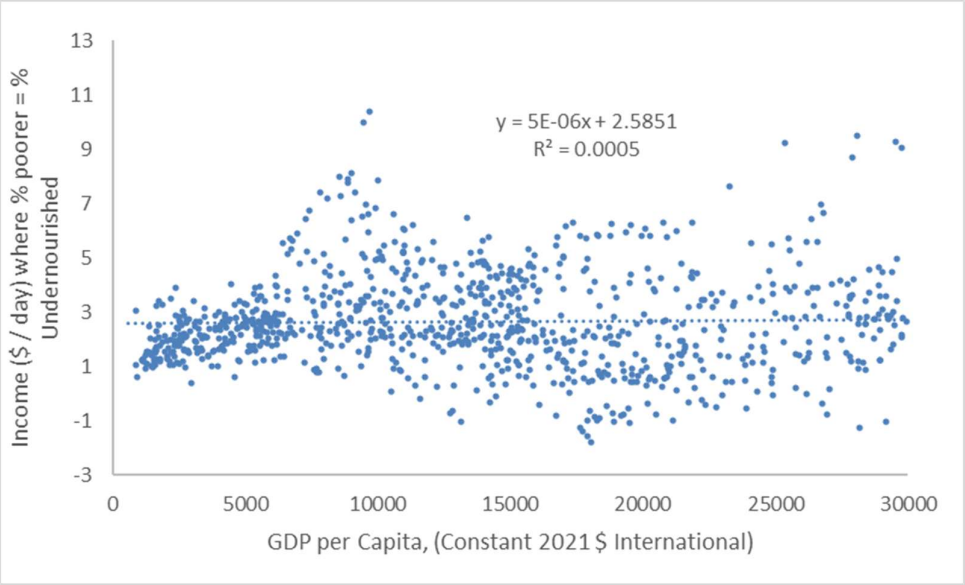

This provides a threshold income ($2.58) above which citizens can afford imported food to mitigate any short-fall in regional food production, and beneath which citizens will be exposed to undernourishment (Figure S6).

Figure S6 Proportion of Population with Income Low Enough for Undernourishment

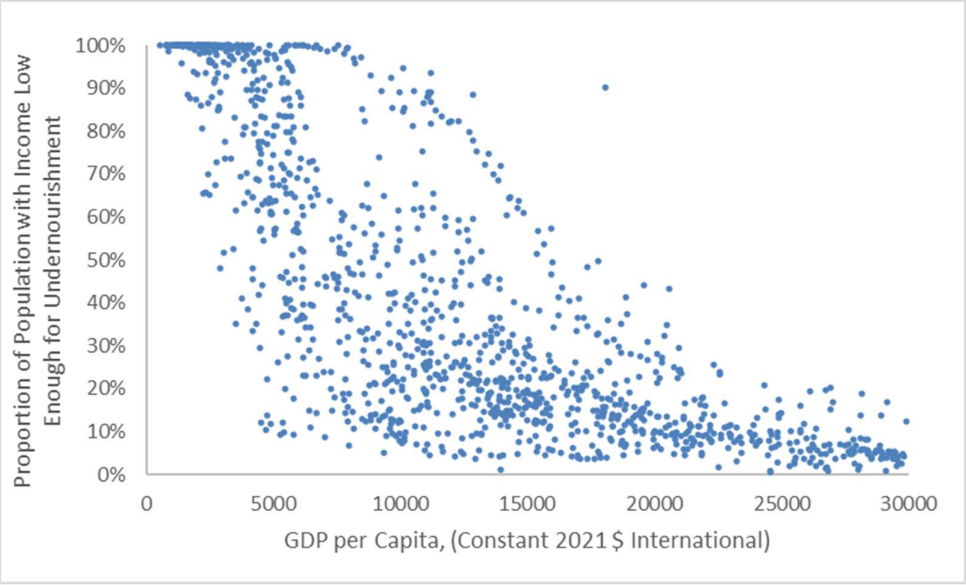

Using the regional compound rate of GDP growth compared to the global rate of GDP growth, we can infer how each region is becoming relatively more or less prosperous. This provides 4 regional conditions:

- Undernourished and getting relatively poorer – no chance of escaping (Regions in Africa and parts of Asia)
- Undernourished and getting relatively richer – undernourishment decreasing with increased prosperity (Regions in parts of Asia and Central America)
- Not undernourished yet but becoming relatively poorer – approaching the income threshold which cannot protect increasing proportions of the poorer citizens from undernourishment in climate vulnerable regions (South America, North America and eventually West Asia)
- Not undernourished and becoming relatively wealthier – regions where the population is economically protected from food insecurity even when that region starts to become climate vulnerable (More established emerging Asian economies)

This was then related to each region's income distribution to estimate the proportion of regional population that is economically exposed to undernourishment. The forecast proportion of undernourishment for each region is then taken as the minimum of the proportion estimated vulnerable to climate caused undernourishment or the estimated proportion of population economically vulnerable.

2.5 Disaster-Related Deaths

The EM-DAT database (Centre, 2023) was analysed to identify disaster classes significantly correlated with atmospheric CO_2. Storms, floods, landslides, and wildfires showed robust associations, while earthquakes, volcanic eruptions, and droughts (to avoid double-counting starvation) were excluded. Regression analysis estimated both disaster frequency and, where plausible, severity (deaths per disaster). Outliers were removed to stabilise averages. Population-normalised data helped distinguish climate drivers from population exposure effects.

2.6 Health Impacts

Climate-attributable deaths from heat and cold extremes, diarrhoea and malaria were reviewed but excluded due to insufficient or inconsistent correlation with CO_2 or GMST in available data.

2.7 Air Pollution

Air pollution deaths from fossil fuel combustion were included for context, though considered coincidental rather than directly climate-driven. Jacobson's (Jacobson, 2008) temperature-based estimates were incorporated.

2.8 Mortality-Emissions Metric

For each scenario, cumulative climate deaths (starvation/conflict, disasters, air pollution) were estimated from 1900 to 2200. These were divided by cumulative CO_2 emissions to produce a deaths-per-megatonne metric. Because deaths reduce to zero as atmospheric CO_2 concentration drops to 350 ppm and emissions drop to zero according to the different zero emission scenarios, cumulative deaths and cumulative emissions both eventually reach asymptotic values. The ratio of these represents the

enduring human cost of fossil fuel emissions – cumulative lives lost per cumulative emission since 1900.

2.9 Uncertainty

Confidence intervals (95%) were calculated for linearized regression-based categories. For starvation and conflict limited data results in very wide confidence limits. Limitations include the exclusion of emerging mortality pathways (unknown unknowns), and the inability of historical data to inform the implications of accelerating compounding climate feedback loops.

The analysis seeks to be as comprehensive as possible but recognises that some categories overlap, data are incomplete or contested, and additional mortality pathways may emerge. Estimates are therefore contingent on available evidence and assumptions, so should be interpreted as indicative and precautionary rather than definitive. Mankind is currently flying blind into the future with no broad ranging, global scope approximate forecast of climate mortality impacts.

S3. Derivation of Combined Development-Driven Decline and Climate-Driven Increase Functions for Undernourishment and Conflict Mortality

This Supplementary Information expands upon the methodology, results, and sensitivity analyses described in the main text [1–17], with all references aligned to the numbering system used there. Where appropriate, additional figures and equations are provided to illustrate supporting detail. In particular, findings are interpreted in the context of the Paris Agreement threshold of net zero emissions by 2050 [16].

3.1 Forecasting Climate-Related Starvation and Conflict Deaths

Extended Methods and Derivations

Here we provide full regression derivations and methodological details excluded from the main text. This includes the separation of development-driven versus climate-driven undernourishment trends, details of the iterative fitting process, and full regression equations (Equations 1–8).

Equations

Equation 1. Population to emissions regression:

$CO_2\ emitted_{year}$ = 0.0057 x World Population Millions - 7.78 Gt

R^2 = 0.99 Standard Range = 1.05 Gt

Equation 2. Emissions S-curve decline function:

$CO_2\ emitted_{year} = \exp(-\text{S-curve factor} \times (\text{Year} - 2030)^2) \times CO_2\ emitted_{2030}$ Gt

Table 1. S-Curve factors for Scenario CO_2 Emissions Decline to Zero

Emissions decline from 2030	to 2050	to 2060	to 2070
S-curve factor	0.015	0.007	0.004

Equation 3. Atmospheric CO_2 concentration dynamics with half-life adjustment:

$CO_2\ conc_{year} = ((CO_2\ conc_{year-1} – CO2\ conc_{preind})/ HLF) + CO_2\ conc_{preind}$ ppm

Where:
$CO_2\ conc_{preind}$ = 280 ppm
Half Life = 72 years
Half-Life Factor (HLF) = exp((ln2/Half-Life) = 1.01 (exponential decay curve)

Equation 4 Quantity of CO_2 removed each year:

$CO_2\ removed_{year} = (CO_2\ conc_{year-1} – CO_2\ conc_{year}) /1000000$ x Mass Atmosphere Gt

Where:
Mass Atmosphere = 5.15 x 106 Gt

Equation 5 CO_2 emitted, net of natural drawdown per year:

CO_2 emitted, net natural $drawdown_{year} = CO2\ emitted_{year} - CO_2\ removed_{year}$ Gt

Equation 6. GMST anomaly versus cumulative CO_2 emissions:

GMST $anomaly_{year} = 0.0009$ x CO_2 emitted net natural $drawdown_{year}$ (Gt) DegC
$R^2 = 0.894$ Standard Range = 0.119 Deg.C

Equation 7. Development-driven decline function for undernourishment/conflict derivation:

To model the decline in undernourishment with time, the following modelling assumptions were made:

Decline in undernourishment and conflict % (Uy) with time is proportional to time (y) and to the proportion still undernourished (i.e. the proportion undernourished approaches but never reaches zero):

$U_y \propto$ time (y) . U_y

$dU_y = y\ .\ U_y\ dy$ (S1)

$dU_y / U_y = y\ .\ dy$ (S2)

$\ln (U_y) = a \,.\, \ln (y) + b$ Equation 7 (S3)

Regression of ln (y) against ln (U_y) gives gradient a and intercept b, but see below for iteration together with co-dependent Climate Driven Increase function.

This curve fits the curve of declining infant mortality extremely well and fits the curve for undernourishment fairly well prior to climate causation being very significant.

Equation 8. Climate-driven increase function for undernourishment/conflict derivation:

To model the increasing undernourishment and conflict deaths due to climate the following modelling assumptions were made:

Climate caused undernourishment and conflict (%) (U_c) increase with CO_2 concentration C and to the proportion still adequately nourished (i.e. the proportion undernourished can never exceed 100%). We use ($C - C_{50}$) where C_{50} is the CO_2 concentration that coincides with 50% of the population being undernourished in order to provide a symmetrical S-curve between 0% and 100%.

$U_c \propto (C - C_{50}) \,.\, (1 - U_c)$

$\ln (1 - U_c) = - d \,.\, (C - C_{50}) \,.\, dC$ Equation 8 (S4)

Regression of ln ($1 - U_c$) against C gives gradient d and C_{50} of – intercept / gradient

Equations 9 and 10. Iteration methodology to provide the constants for the separated U_y and U_c functions:

The data that we have is for the total (U_f) of declining undernourishment with time (U_y) PLUS the increasing undernourishment with CO_2 (U_c)

The U_y and U_c functions should fit best at the opposite extremes:

for U_y, in earlier times where the influence of climate is minimal compared to the improvement with development and

for U_c where climate effects have long overtaken the development improvements with time and

at the cross-over point (~2015), $U_y = U_c = 1/2\ U_f$ (S5)

To distinguish the two curves depicting U_y and U_c, accepting our modeliing constraints, we can iterate a solution:

Initially let:

new U_y = U_f (actual data) – first pass modelled estimate of $U_c/2$ (S6)

new U_c = U_f (actual data) – first pass modelled estimate of $U_y/2$ (S7)

This makes:

new $U_y \rightarrow U_f$ as $U_c \rightarrow 0$

new Uc → Uf as $U_y \rightarrow 0$

new U_y → new $U_c = U_f / 2$ as $U_c \rightarrow C_{50}$ (S8)

new U_c → new $U_y = U_f / 2$ as $U_y \rightarrow C_{50}$ (S9)

But these values no longer meet our modelling curve constraints – so these points can now be remodelled for best-fit to the modelling curve constraints to obtain first iteration U_y and U_c.

Now we can refine first iteration U_y and U_c as:

newer $U_y = (2*(U_f$ – new $U_c/2)$ + new$U_y)/3$ (S10)

newer $U_c = (2*(U_f$ – new $U_y/2)$ + new$U_c)/3$ (S11)

But these values no longer meet our modelling curve constraints – so these points can now be remodelled for best-fit to the modelling curve constraints to obtain next iteration U_y and U_c.

For the undernourished plus conflict deaths data, the best fit for the two curves to the actual data (U_f) was obtained by the second iteration and further iterations oscillated either side of the best fit solution.

Finally, by trial and error the best fit curves were obtained resulting in the factors in table 2 to be used with Equations 9 and 10:

$U_y (\%) = \exp(A . \ln (y) + B)$ Equation 9 (S12)

$U_c (\%) = 1 / (1 + \exp(- D . (C + E / 0.0533)))$ Equation 10 (S13)

[This equation is second order in C. A similar approach using a linear relationship with C (first order) gives smaller forecasts of climate caused deaths, but could not match the smooth transition from U_y to U_c seen in the real data and has problematic boundary conditions – below a lower threshold of CO_2 concentrations U_c would be negative (trapped at zero to estimate deaths) and above an upper threshold of CO_2 concentrations Uc would exceed 100% (trapped at 100% to estimate deaths).]

Table 2 Factors to be Used with Equations 9 and 10:

Region	Ny - Factors					Nc - Factors					C50%
	A	B	R2	St.d Range	Pearson	D	E	R2	St.d Range	Pearson	ppm
Eastern Africa	-175	1324	0.91	0.11	-0.95	0.0300	-18.4	0.89	0.064	0.945	614
Middle Africa	-156	1182	0.79	0.14	-0.89	0.0251	-16.5	0.94	0.048	0.968	658
Northern Africa	-119	894	0.75	0.12	-0.86	0.0224	-16.8	0.83	0.076	0.909	750
Southern Africa	-89	671	0.57	0.07	-0.75	0.0290	-19.0	0.82	0.152	0.905	655
Western Africa	-191	1442	0.98	0.03	-0.99	0.0150	-13.1	0.89	0.048	0.942	870
Central America	No Data	No Data	No Data	No Data	No Data	0.0233	-16.3	0.80	0.092	0.892	698
North America	145	-1108	No Data	No Data	1.00	0.0382	-23.9	0.80	0.092	0.892	625
South America	-270	2049	0.96	0.13	-0.98	0.0596	-32.1	0.76	0.184	0.874	538
Central Asia	No Data	No Data	No Data	No Data	No Data	0.0355	-22.5	0.80	0.092	0.892	634
Northern Asia	-657	4985	1.00	No Data	-1.00	0.0432	-26.5	0.80	0.092	0.892	612
Southern Asia	-105	793	0.86	0.12	-0.93	0.0414	-24.1	0.98	0.024	0.989	582
Western Asia	-194	1466	0.94	0.08	-0.97	0.0351	-21.1	0.57	0.243	0.754	601
Eastern Asia	-351	2661	0.89	0.22	-0.94	0.0316	-20.5	0.80	0.092	0.892	649
South-eastern Asia	No Data	No Data	No Data	No Data	No Data	0.0226	-15.9	0.80	0.092	0.892	704
Caribbean	-100	757	0.81	0.11	-0.90	0.0266	-17.8	0.89	0.052	0.943	671
Eastern Europe	-348	2640	0.92	0.09	-0.96	0.0380	-23.8	0.80	0.092	0.892	626
Northern Europe	0	-9	No Data	No Data	No Data	0.0428	-26.2	0.80	0.092	0.892	613
Southern Europe	0	-9	No Data	No Data	No Data	0.0343	-21.9	0.80	0.092	0.892	638
Western Europe	0	-8	No Data	No Data	No Data	0.0378	-23.7	0.80	0.092	0.892	626
Melanesia	-50	376	0.55	0.10	-0.74	0.0120	-11.5	0.52	0.064	0.721	959
Micronesia	No Data	No Data	No Data	No Data	No Data	0.0195	-14.3	0.80	0.092	0.892	735
Oceania	-56	420	0.68	0.09	-0.82	0.0170	-14.8	0.74	0.056	0.859	867

Derivations and fitting parameters are provided in full here for transparency.

S4 Sensitivity Analyses

We tested the robustness of results to alternative assumptions:
- Different functional forms for regression (first order vs second order).

- Separate modelling of conflict deaths from undernourishment deaths

- Alternative causation to climate (CO_2 concentration as proxy) for undernourishment and conflict to 151 potential alternatives:

These analyses confirm climate (CO_2 concentration as proxy) as the most viable underlying cause of undernourishment and conflict deaths.